SOIL DEFORMATION RATES AND ACTIVATION ENERGIES

Thesis for the Degree of Ph. D.
MICHIGAN STATE UNIVERSITY
ARTHUR GORDON DOUGLAS
1969

This is to certify that the

thesis entitled

SOIL DEFORMATION RATES AND
ACTIVATION ENERGIES.

presented by

Arthur Gordon Douglas

has been accepted towards fulfillment
of the requirements for

Ph.D. degree in Civil Engineering

O. B. Andersland

Major professor

Date February 21, 1969.

ABSTRACT

SOIL DEFORMATION RATES AND ACTIVATION ENERGIES

By

Arthur Gordon Douglas

The free energy of activation of flow for Sault Ste. Marie clay has been determined by the application of the absolute reaction rate theory. The viscous flow of dilute soil-water mixtures and the steady state creep of consolidated samples were considered.

The viscosity of the soil-water mixtures increased slowly as the concentration of solids was increased until there were sufficient solids to form a continuous structure. At this point the mixture became thixotropic. The rate at which the viscosity increased was dependent upon the nature of the adsorbed ions. The highly hydrated lithium ion caused a more rapid increase than the less hydrated potassium ion. This is considered to be due to the increased effective size of the particles.

The free energy of activation of the dilute suspensions was found to be independent of the concentration and equal to that of pure water. It is concluded that the flow mechanism is that of free water in a porous medium and that the isolated clay particles make no contribution to the free energy.

Creep tests on consolidated samples were conducted at constant temperature with several increments of axial stress. These tests indicate that the free energy of activation for this soil is approximately 28 K. calories/mole and is independent of the nature of the adsorption complex. Also, the volume of the flow unit was calculated to be 1.7 cubic angstroms. These results suggest that the bonding mechanism is not related to the adsorbed water layer and is in the form of ionic bonds at points of direct mineral to mineral contact.

SOIL DEFORMATION RATES AND ACTIVATION ENERGIES

By

Arthur Gordon Douglas

A THESIS

Submitted to
Michigan State University
in partial fulfillment of the requirements
for the degree of

DOCTOR OF PHILOSOPHY

Department of Civil Engineering

1969

ACKNOWLEDGMENTS

The writer wishes to express his deep appreciation to his major professor, Dr. O. B. Andersland, Professor of Civil Engineering, for his aid and encouragement throughout the writer's doctoral studies and for his help and guidance in the preparation of this thesis. Thanks are also due the other members of the writer's doctoral committee: Dr. M. M. Mortland, Professor of Soil Science; Dr. R. K. Wen, Professor of Civil Engineering; and Dr. L. E. Malvern, Professor of Applied Mechanics.

Thanks go to the National Science Foundation and the Division of Engineering Research at Michigan State University for the financial assistance that made these studies possible.

TABLE OF CONTENTS

LIST OF TABLES

LIST OF FIGURES

NOTATIONS

$\mathring{A}$ = angstrom units = 10^{-8} cm.

a = shape factor

D = dielectric constant

E = allowable energy levels of a particle

ΔE = quantum of energy

E_x = experimental activation energy

ΔF = free energy of activation

g = degeneracy

ΔH = enthalpy of activation

h = Planck's constant = 6.624×10^{-27} erg. sec.

K = equilibrium constant

k = Boltzmann's constant = 1.3805×10^{-16} erg/degree molecule

k' = rate constant

L = applied force

m = mass of a particle

m_1, m_2 = dipole moments

N_A = number of molecules in all energy levels of A

n_i = number of particles at energy level E_i

P = electric potential

Q = attractive potential

Q_A = partition function

R = universal gas constant = 1.987 cal/degree mole

ΔS = entropy of activation

T = absolute temperature ° Kelvin.

t = time

U = potential energy

V_f = flow volume

Z = valency

γ = shear strain

$\dot{\gamma}$ = rate of shear strain

δ = horizontal displacement

$\dot{\varepsilon}$ = natural axial strain rate

ψ = wave function

λ = distance between equilibrium positions.

η = coefficient of viscosity

ϕ = concentration of soil

σ_1 = major principal stress

σ_3 = minor principal stress

σ_{oct} = octahedral stress

τ = octahedral shear stress

ν = frequency of vibration

CHAPTER I

INTRODUCTION

The mechanisms of viscosity, plasticity, and diffusion are now accepted as examples of the theory of absolute reaction rates as formulated by Glasstone, Laidler and Eyring (1941). In recent years, this theory has been applied to the study of time-dependent deformation of both liquids and solids. Attempts have also been made to apply the theory to the creep of both frozen and unfrozen soil. This research is still in its preliminary stages, but the results obtained indicate that the creep of soils can be treated as a thermally activated process.

The theory of absolute reaction rates concerns the movement of particles of atomic size from one equilibrium position to another by surmounting an energy barrier. The magnitude of this barrier is the "free energy of activation" and is the factor which controls the rate of any process in which matter rearranges itself. It is probable that some particles will pass through a barrier instead of surmounting it and this action is known as tunneling. The proportion of the total number of particles involved in tunneling is small and this mechanism is not considered in the development of the equations presented.

The rate equations are derived from quantum mechanics and are based upon the distribution of thermal energies between atomic particles. Despite many superficial similarities, they are not applicable to a mass of soil particles. For while there is an energy barrier restraining a grain from moving from one equilibrium position to the next, such movement requires the direct application of a mechanical force. This is a mechanically activated process, and must be distinguished from a thermally activated process. It will be shown that when the flow of a soil mass is considered, the energy which is used in overcoming the mechanical resistance must be deducted in order to determine the free energy of activation due to surface forces. In saturated clays this mechanical energy is negligible but in sands it is the dominant term.

In an equilibrium situation, particles which have sufficient energy cross the energy barrier with equal frequency in both directions. A flow process will be induced if the shape of the barrier is distorted by the application of a directed potential so that the height from one side is less than from the other side causing a greater net flow in one direction than in the reverse direction. Since the rate of flow is controlled by the height of the barrier and the thermal energy of the particles, the free energy of activation may be found by observing the change in the flow rate at constant stress with a change in temperature. This is a convenient

method for use with viscosity tests on fluids but with solid materials undergoing creep it has the disadvantage that continuous structural changes are taking place and the temperature change can not be induced instantaneously. For this reason the method which was developed here was to apply a small increment of stress to a sample undergoing steady state creep and observe the change in the creep rate. The free energy of activation could then be calculated from two simultaneous equations.

The application of the rate theory to liquids and metals has led to a greater understanding of flow mechanisms. In general, there are two factors involved. The particle must make a hole for itself as it moves forward and it must break the bonds with which it is attached to its neighbors. The energies which have been measured for a great many materials are less than those required to form a hole of molecular size and so it is concluded that holes already exist in all materials and that the particle only has to enlarge an existing hole. It has been found that for many materials, the ratio of the energy required to enlarge a hole to the energy required to form a hole is about 0.25 (Glasstone, Laidler and Eyring, 1941). For non-associated liquids, the enlargement of the holes accounts for most of the free energy of activation but for associated liquids such as water, a relatively large proportion is used in breaking the hydrogen bonds.

The experimental results indicate that both changes in the adsorbed ion and dehydration followed by saturation with carbon tetrachloride had no effect on the value of the free energy of activation. This indicates that ionic bonding between particles is a major factor in the rate controlling mechanism. Further support for this view is provided by the fact that the magnitude of the calculated value of the free energy of activation is in the range of strengths of ionic bonds.

CHAPTER II

REVIEW AND THEORY

Flow Processes

In very dilute concentrations, soil-water mixtures exhibit typical Newtonian flow characteristics as illustrated in Figure 2-1a and the coefficient of viscosity η may be represented by the Einstein equation [Baver, 1956]

$$\eta = \eta_o (1 + a\phi) \qquad (2\text{-}1)$$

where η_o is the coefficient of viscosity of the fluid, ϕ is the concentration of the particles and "a" is a shape factor. As the concentration of solids is increased and interaction occurs between the particles, the flow becomes thixotropic as illustrated in Figure 2-1b, and becomes both rate and time dependent. The variation of the yield stress with water content as determined by this method for sodium and hydrogen saturated kaolinite is shown in Figure 2-1c [Scott, 1963].

Compacted soils also exhibit time-dependent deformation under constant stress and temperature. The basic features of typical creep curves are illustrated in Figure 2-2. In the general case, a creep curve consists of four

stages: Stage I, termed the "instantaneous strain," represents the strain which occurs on loading; Stage II, termed the "primary" or "transient" creep, represents the initial region of decreasing creep rate; Stage III, termed "secondary" or "steady-state" creep, represents the region of relatively constant creep rate; Stage IV, termed the "tertiary" creep, represents the final stage leading to failure. One or more of these stages may not occur at certain stress levels in a particular specimen. At low stress levels, Stages III and IV do not occur and the creep is said to be damped. If the stress exceeds the limiting value, Stages III and IV do occur and the creep is said to be undamped.

Variations in the creep rate are considered to be the result of the simultaneous operation of weakening and strengthening processes. When the strengthening process predominates, the rate decreases (primary creep); when the strengthening and weakening processes are equal, the rate is constant (secondary creep); and if the weakening process predominates the rate increases and leads to failure (tertiary creep).

Physicochemical Properties of Clays

The strengthening and weakening processes involved in the flow of clays depend upon the inter-particle forces which exist as a consequence of the mineralogical structure of the clay. The structure of the four minerals mentioned

in this project is illustrated in Figure 2-3 [Grim, 1953]. At the edges of the sheets, the continuity of the structure is broken and a net negative charge is produced although local concentrations of positive charges may occur. Negative charges may also be produced on the surfaces by isomorphous substitution of lower valence ions for the silicon and aluminum in the tetrahedral and octahedral sheets.

The net negative charge tends to attract the positive hydrogen ions in the water and develops a degree of orientation in the molecules close to the surface. The degree of orientation and the thickness of this adsorbed layer are uncertain. Low and Anderson [1958] in two reviews of experiments with bentonite found no evidence of orientation at a distance of 84Å but at 12Å the water had a density of 0.97 g./c.c. compared to 0.99987 for water at 0°C. and 0.917 for ice at 0°C. It is therefore suggested that the first layer of water molecules is rigidly held, and possibly hydrogen bonded to the surface, and that the degree of orientation decays rapidly away from the surface.

If any metallic cations are present in solution, they are also attracted towards the negatively charged surface and come to an equilibrium position where the attraction to the surface is balanced by their mutual repulsion and form a mobile cloud near the surface. The negatively charged plate and the positively charged cation cloud form

a system known as the "diffuse double layer." The electric potential P at a distance x from the surface may be expressed by a simplified form of the Guoy-Chapman equation as:

$$P = \frac{4kT}{Z\epsilon} \exp. \left(\frac{8\pi\phi\epsilon^2 Z^2 x}{DkT}\right) \qquad (2\text{-}2)$$

where k is Boltzmann's constant, T is the absolute temperature, Z is the valency, ϵ is the electrostatic unit of charge and D is the dielectric constant.

Verwey and Overbeek [1948] attributed the attractive forces between clay particles to van der Waal's forces and derived the following equation for the attractive potential Q between two dipoles:

$$Q = \frac{C}{3} \frac{m_1^2 m_2^2}{DkTx^6} \qquad (2\text{-}3)$$

where C is a constant and m_1, m_2 are the two dipole moments. Thus the attractive potential varies inversely as the sixth power of the distance while the repulsive potential varies inversely as an exponential function of the distance. The result of the combination of these two potentials is illustrated in Figure 2-4.

Molecular Energies

The clay and water molecules are in a constant state of thermal agitation with an intensity which depends upon the environmental temperature. Each molecule, however, is held to its neighbours by bonds which are strong in the case of the clay crystal and weak in the case of water. Periodically, a molecule may attain sufficient energy to break its bonds and move to another equilibrium position. If a stress is applied to the system, the energy barriers will be altered and movement will tend to occur in a preferred direction. The nature and magnitude of the molecular energies is therefore a prime factor in the consideration of the mechanism of flow.

The view that the energy of particles was "quantized" and that only certain discrete energy levels were allowed was suggested by Max Planck [1900] when he proposed the following relation:

$$\Delta E = h\nu \qquad (2\text{-}4)$$

where ΔE is the quantum of energy emitted when an oscillating particle moves to the next lower energy level, h is a constant known as Planck's constant and has the value 6.624×10^{-27} erg. sec. and ν is the frequency of the radiation emitted. Niels Bohr's description of the atom [1913] was based upon this equation but although this description gave many acceptable results, it failed

as a complete description because it did not recognize the simultaneous corpuscular and wave nature of matter. This was considered by Erwin Schroedinger [1926] who suggested that the behavior of particles of atomic dimensions may be calculated from a wave equation, which for a particle restrained to the x axis is:

$$E\psi = -\frac{h^2}{8\pi^2 m}\frac{d^2\psi}{dx^2} + U(x)\psi \qquad (2\text{-}5)$$

where E represents the allowable energy levels of the particle, ψ is a wave function, a function of x such that ψ^2 is the probability of the particle being at various distances along the x axis, m is the mass of the particle and U(x) is the potential energy. In the region $o < x < a$, the potential is constant and may be taken as datum, so that in that region, equation (2-5) becomes:

$$E\psi = -\frac{h^2}{8\pi^2 m}\frac{d^2\psi}{dx^2} \qquad (2\text{-}6)$$

Functions which solve this equation are:

$$\psi = A \sin\frac{n\pi x}{a} \quad \text{where } n = 1, 2, 3, \cdots \qquad (2\text{-}7)$$

and A is a constant. Hence,

$$E = \frac{n^2h^2}{8ma^2} \qquad n = 1, 2, 3 \cdots \qquad (2\text{-}8)$$

The solutions in three dimensions are obtained by taking equations (2-7) and (2-8) in each of the co-ordinate directions. Then,

$$\psi = (\psi_x)\ (\psi_y)\ (\psi_z) \qquad (2\text{-}9)$$

and

$$E = E_x + E_y + E_z$$

These equations are difficult to understand in terms of ordinary sized particles but the following observations may be made.

(i) There are certain positions where the probability of finding the particle is zero.

(ii) Only certain discrete energy levels are possible.

(iii) A particle may not have zero energy

(iv) The more closely a particle is confined, the greater the spacing of the allowed energy levels.

Also, if only one electron in each atom or molecule may be in an excited state, the energy of an Avagadro's number of these atoms or molecules is $21.6n^2$ kilo calories/mole. Hence the allowed energy levels for electrons in atoms or

molecules are very widely spaced compared with ordinary thermal energies.

The distribution of particles through the various allowed energy levels was given by Boltzmann as:

$$n_i/n_o = \exp. (-\Delta E_i/kT) \qquad (-10)$$

where n_i is the number of particles at energy level E_i, n_o is the number of particles at energy level E_o and k is Boltzmann's constant equal to 1.380×10^{-16} erg./degree molecule. The appearance of the term kT in this expression is of particular significance. It indicates that if a molecule possesses energy in excess of the lowest allowable level, this excess, which is known as "thermal energy," is dependent upon the temperature of the system. The allowed energies in a cubic container are given by:

$$E = (n_x^2 + n_y^2 + n_z^2) \frac{h^2}{8ma^2} \qquad (2-11)$$

The total number of combinations of values of n_x, n_y and n_z corresponding to the same energy state is called the "degeneracy" denoted by "g" so that

$$\frac{n_i}{n_o} = g \exp. (-\Delta E_i/kT) \qquad (2-12)$$

Molecules may possess thermal energy due to motion in the form of vibration, rotation or translation. The average translational energy of an Avagadro's number of molecules is 1/2 RT per degree of freedom where R is the universal gas constant. Each molecule is free to rotate about each of the co-ordinate axes and hence has three rotational degrees of freedom. A linear molecule, however, has no rotational energy about its axis. The average rotational energy is 1/2 RT per degree of freedom and hence for linear molecules becomes RT and for non-linear molecules becomes 3/2 RT. Each atom in a molecule has three degrees of freedom and hence the total number of degrees of freedom for a molecule of n atoms is 3n. For a non-linear molecule there are three degrees of translation and three degrees of rotation so that the number of degrees of vibrational freedom is 3n-6. Of particular interest here is the H_2O molecule which is non-linear with an internal angle of 105°. With three atoms it is seen to have three degrees of vibrational freedom as shown in Figure 2-5. The thermal energy of a non-linear molecule is then given by

$$E - E_o = 5/2\ RT + E_{vib.} \qquad (2\text{-}13)$$

Rate Process Theory

For many simple chemical reactions of the type

$$nA \rightarrow B$$

the rate at which the reaction occurs is given by $k'(A)^n$ and the reaction is designated as first, second or third order depending upon whether n is 1, 2 or 3. k' is called the rate constant. Only second order reactions will be considered.

The equilibrium constant K for the reaction

$$A \rightleftarrows B$$

is given by

$$K = \frac{N_B}{N_A} \tag{2-14}$$

where N_A and N_B represent the number of molecules in all of the energy levels of A and B respectively. So that from equation (2-10)

$$K = \text{exp. } (-\Delta E_o/kT) \frac{E \text{ exp. } (-iE_B/kT)}{E \text{ exp. } (-iE_A/kT)} \tag{2-15}$$

which may be written as

$$K = \text{exp. } (-\Delta E_o/kT) \frac{Q_B}{Q_A} \tag{2-16}$$

where Q_A and Q_B are known as "partition functions."

According to the transition state theory as developed by Glasstone, Laidler and Eyring [1941], when two species A and B react, a transition activated state is formed so that

$$A + B \rightarrow (AB)^* \rightarrow \text{products}$$

and the rate of the reaction depends upon the concentration of the activated species and the rate at which it breaks up. The equilibrium constant for the activated state according to equation (2-16) is:

$$K^* = \frac{Q_{(AB)^*}}{Q_A\, Q_B} \quad \exp.\ (-\Delta E_o^*/RT) \qquad (2\text{-}17)$$

hence

$$k' = \frac{Q_{(AB)^*}}{Q_A\, Q_B} \quad \exp.\ (-\Delta E_o^*/RT) \qquad (2\text{-}18)$$

which may be written as

$$k' = A \exp.\ (-E_a/RT) \qquad (2\text{-}19)$$

and is known as the Arrhenius equation. E_a is called the "activation energy."

An alternative form of equations (2-18) and (2-19) may be obtained by considering that the average vibrational energy of the bonds in the activated complex is given by

kT and the vibrational mode that breaks the complex is given by Plancks equation (2-4). Hence

$$h\nu = kT$$

or

$$\nu = kT/h \qquad (2\text{-}20)$$

the rate of reaction is equal to

$$K^* \frac{kT}{h} (A)(B)$$

hence

$$k' = K^* \frac{kT}{n} \qquad (2\text{-}21)$$

The "free energy of activation" is given by:

$$(\Delta E^\circ)^* = -RT \ln K^*$$

or

$$K^* = \exp. (-(\Delta F^\circ)^*/RT) \qquad (2\text{-}22)$$

and since

$$(\Delta F^\circ)^* = (\Delta H^\circ)^* - T(\Delta S^\circ)^*$$

where $(\Delta H^\circ)^*$ is the "enthalpy of activation" and $(\Delta S^\circ)^*$ is the "entropy of activation"

$$K^* = \exp\left((\Delta S^\circ)^*/R\right) \exp.\ \left(-(\Delta H^\circ)^*/RT\right) \qquad (2\text{-}23)$$

and

$$k' = \frac{kT}{h} \exp.\ \left((\Delta S^\circ)^*/R\right) \exp.\ \left(-(\Delta H^\circ)^*/RT\right) \qquad (2\text{-}24)$$

so that in equation (2-19) the constant A becomes

$$A = \frac{kT}{h} \exp.\ \left((\Delta S^\circ)^*/R\right) \qquad (2\text{-}25)$$

Creep as a Rate Process

The concept of the free energy of activation forming an energy barrier which restricts relative movement of flow units is illustrated in Figure 2-6. The equilibrium condition is shown by curve A and the application of a directed potential, such as a shear force, distorts the curve to position B. The horizontal displacement δ represents the elastic strain and the difference in level of adjacent minima becomes $\tau A\lambda$ where τ is the shear stress, A is the area of the flow unit and λ is the distance between equilibrium positions of the unit. Thus the level of each minimum is altered by $\tau A\lambda/2$.

From equations (2-21) and (2-22)

$$k' = \frac{kT}{h} \exp.\ \left(-\Delta F^\circ/RT\right) \qquad (2\text{-}26)$$

and when the barrier height in the direction of the force becomes $(\Delta F - \tau A\lambda/2)$ and in the direction opposite

the force ($\Delta F + \tau A\lambda/2$). The net rate of activation in the direction of the force is given by

$$\vec{k}' - \overleftarrow{k}' = 2 \frac{kT}{h} \exp. (-\Delta F/RT) \sinh (\tau A\lambda/2kT) \quad (2\text{-}27)$$

The net rate of flow in the forward direction resulting from the applied shear stress is the net specific rate of movement of the flow unit multiplied by the distance λ traversed per movement. Dividing this value by λ_1, the distance between flow units normal to the direction of flow gives the rate of shear strain.

$$\dot{\gamma} = \frac{2\lambda}{\lambda_1} \frac{kT}{h} \exp. (-\Delta F/RT) \sinh (\tau A\lambda/2kT) \quad (2\text{-}28)$$

As a reasonable approximation, $\lambda = \lambda_1$ [Herrin and Jones, 1963], hence equation (2-28) becomes,

$$\dot{\gamma} = \frac{2kT}{h} \exp. (-\Delta F/RT) \sinh (\tau V_f/2kT) \quad (2\text{-}29)$$

where V_f is the volume of the flow unit.

If the energy supplied by the action of the shear force is small compared to the thermal energy,

$$\sinh (\tau V_f/2kT) \simeq \tau V_f/2kT$$

hence equation (2-29) becomes

$$\dot{\gamma} = \tau \frac{V_f}{h} \exp. (-\Delta F/RT) \qquad (2\text{-}29a)$$

that is, the shear rate is proportional to the shear stress which constitutes Newtonian flow. Thus the coefficient of viscosity is given by

$$\eta = \frac{h}{V_f} \exp. (\Delta F/RT) \qquad (2\text{-}30)$$

For the flow of soils and solids however, the energy supplied by the action of the shear stress will be greater than the thermal energy and

$$\sinh (\tau V_f/2kT) \simeq 1/2 \exp. (\tau V_f/2kT)$$

hence equation (2-29) becomes

$$\dot{\gamma} = \frac{kT}{h} \exp. (-\Delta F/RT) \exp. (\tau V_f/2kT) \qquad (2\text{-}31)$$

It is this form which is most useful in the study of the creep process.

Mitchell, Campanella and Singh [1968] modified equation (2-31) to

$$\dot{\varepsilon} = X \exp. (-E_x/RT) \qquad (2\text{-}32)$$

where $\dot{\varepsilon}$ is the axial strain rate and

$$E_x = \Delta F - \tau V_f/2 \qquad (2\text{-}33)$$

where E_x is called the "experimental activation energy." Then from equation (2-32)

$$\frac{\partial \ \ell n \ (\dot{\varepsilon}/T)}{\partial \ (1/T)} = -E_x/R \qquad (2\text{-}34)$$

By observing the steady state creep rate at several temperatures it was possible to plot $\ell n(\dot{\varepsilon}/T)$ against $(1/T)$ for several soils and establish that the relationship was linear as predicted by the theory. Values for E_x were obtained by means of equation (2-34) and for San Francisco Bay mud consolidated at 1 kg./sq. cm. and at a deviator stress of 0.45 kg./sq. cm. a value of 31.4 k. calories/mole was obtained. Also, from equation (2-33) a linear relationship should exist between E_x and τ. Tests on remoulded illite verified this relationship and by extrapolation to $\tau = 0$ ΔF was found to be 43.5 k. calories/mole.

The behavior of polycrystalline ice was investigated by Dillon and Andersland [1967] who found an enthalpy of activation of 11.4 k. calories/mole and the following values of ΔF.

Temp. °C	$\tau_{oct.}$ (psi)	ΔF (k. cal./mole)
-10	120	28.4
-10	100	22.8
-10	90	19.9
- 4	100	28.0
- 4	90	24.7

Goughnour and Andersland [1968] extended this investigation to sand-ice systems and found that ΔF varied with sand concentration as shown in Figure (2-7). Earlier work by Andersland and Akili [1967] on frozen Sault Ste. Marie clay, which is predominantly illite, found ΔF to be of the order of 94 k. calories/mole.

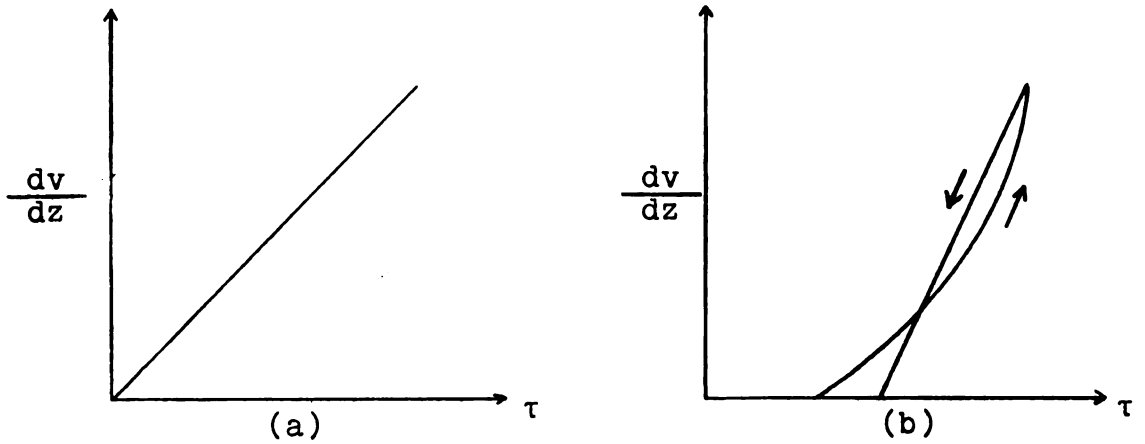

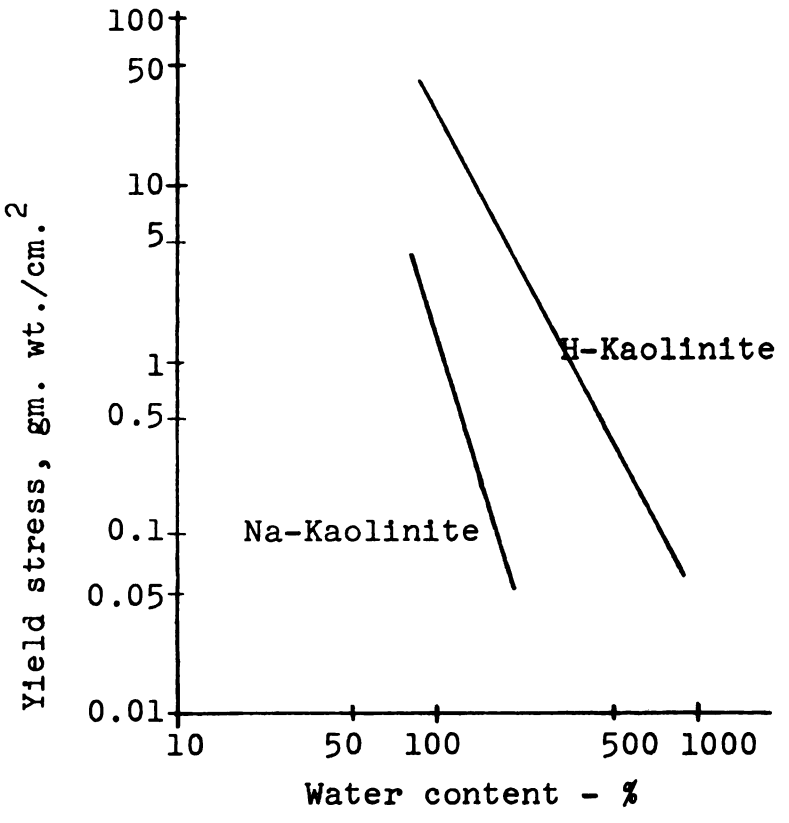

(c)
Variation of yield stress with water content

Fig. 2-1. Rheological properties indicated by viscosity tests.

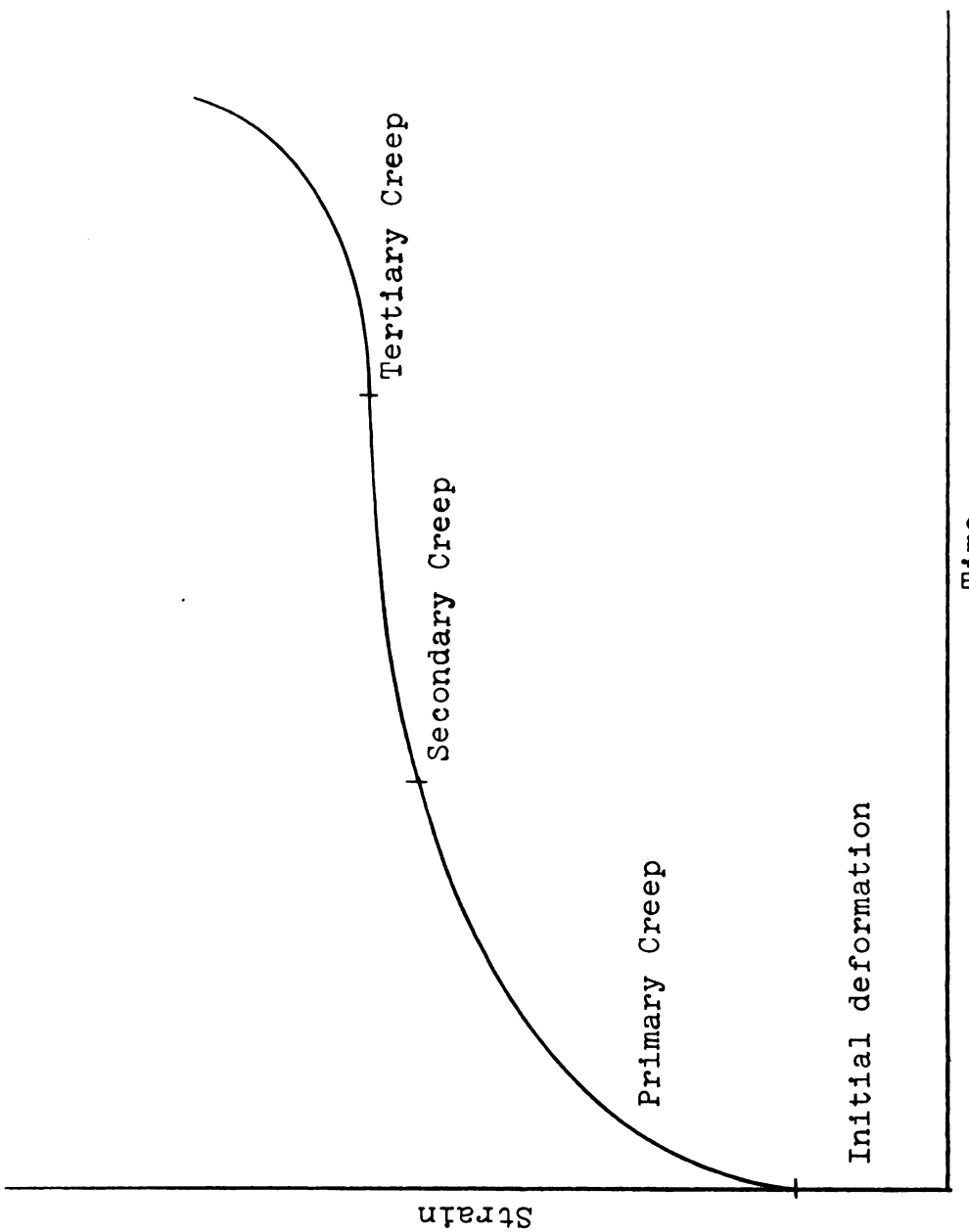

Fig. 2-2. Typical creep curve.

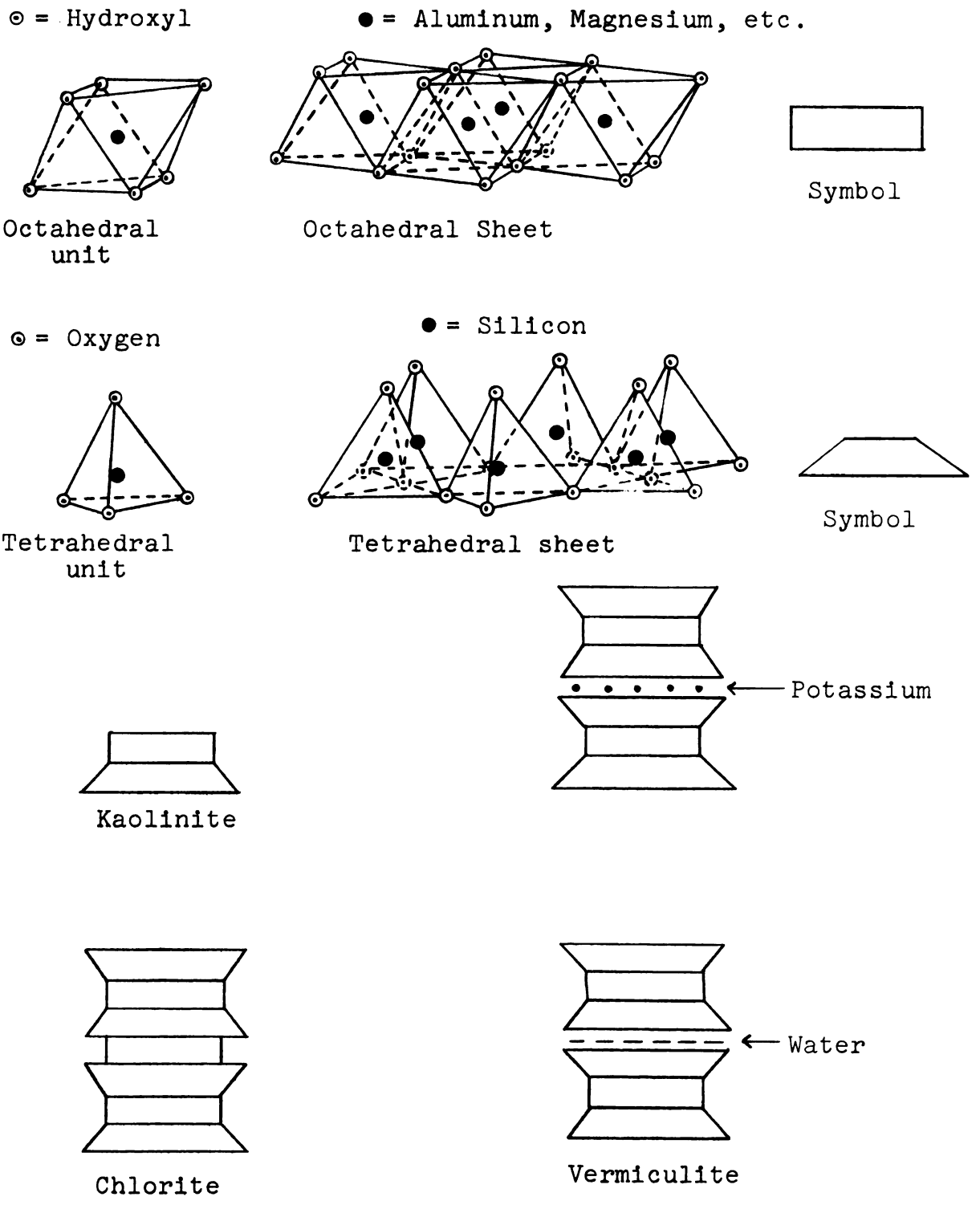

Fig. 2-3. Structure of minerals.

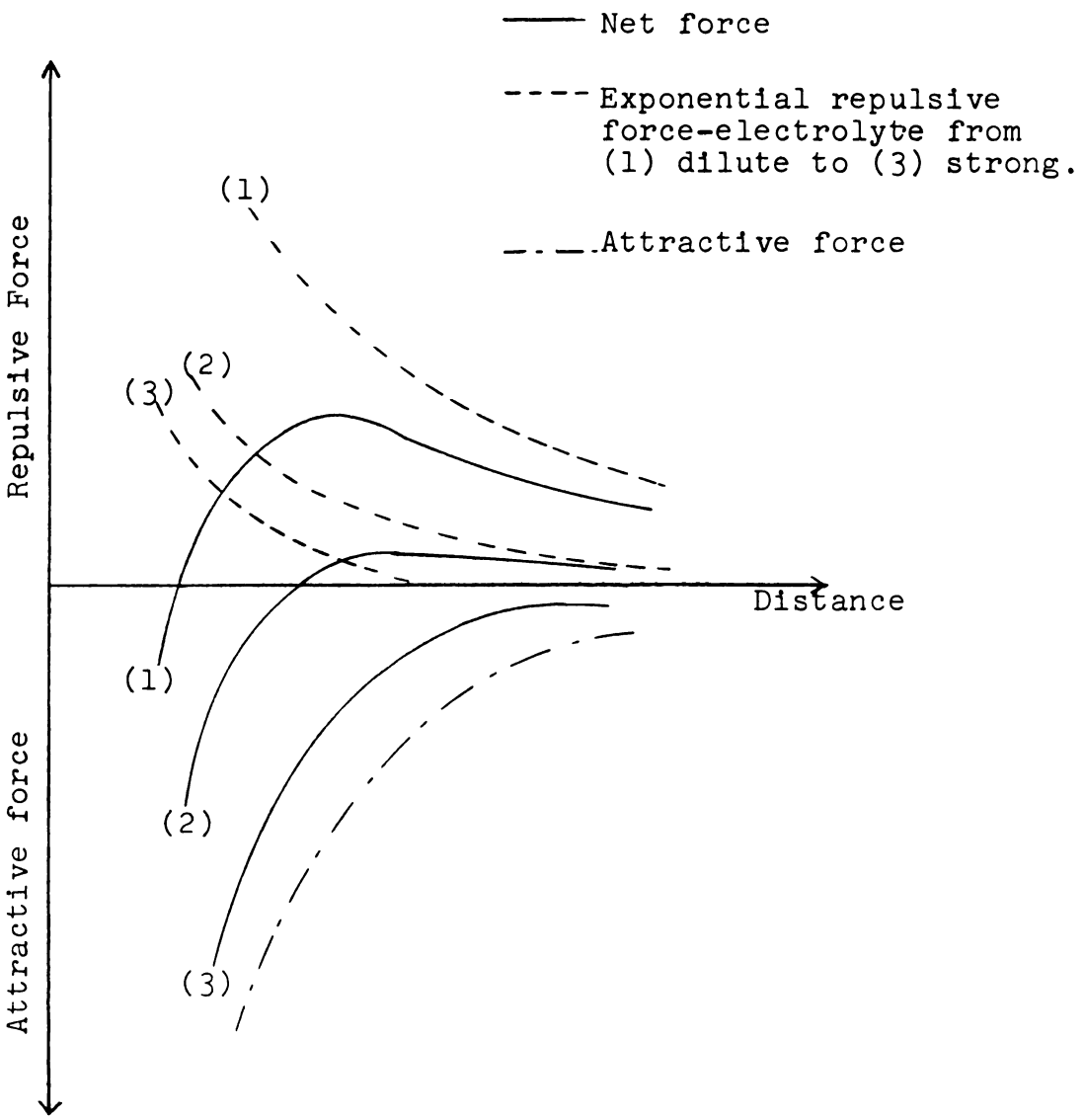

Fig. 2-4. Attraction and repulsion between surfaces (after Scott, 1963).

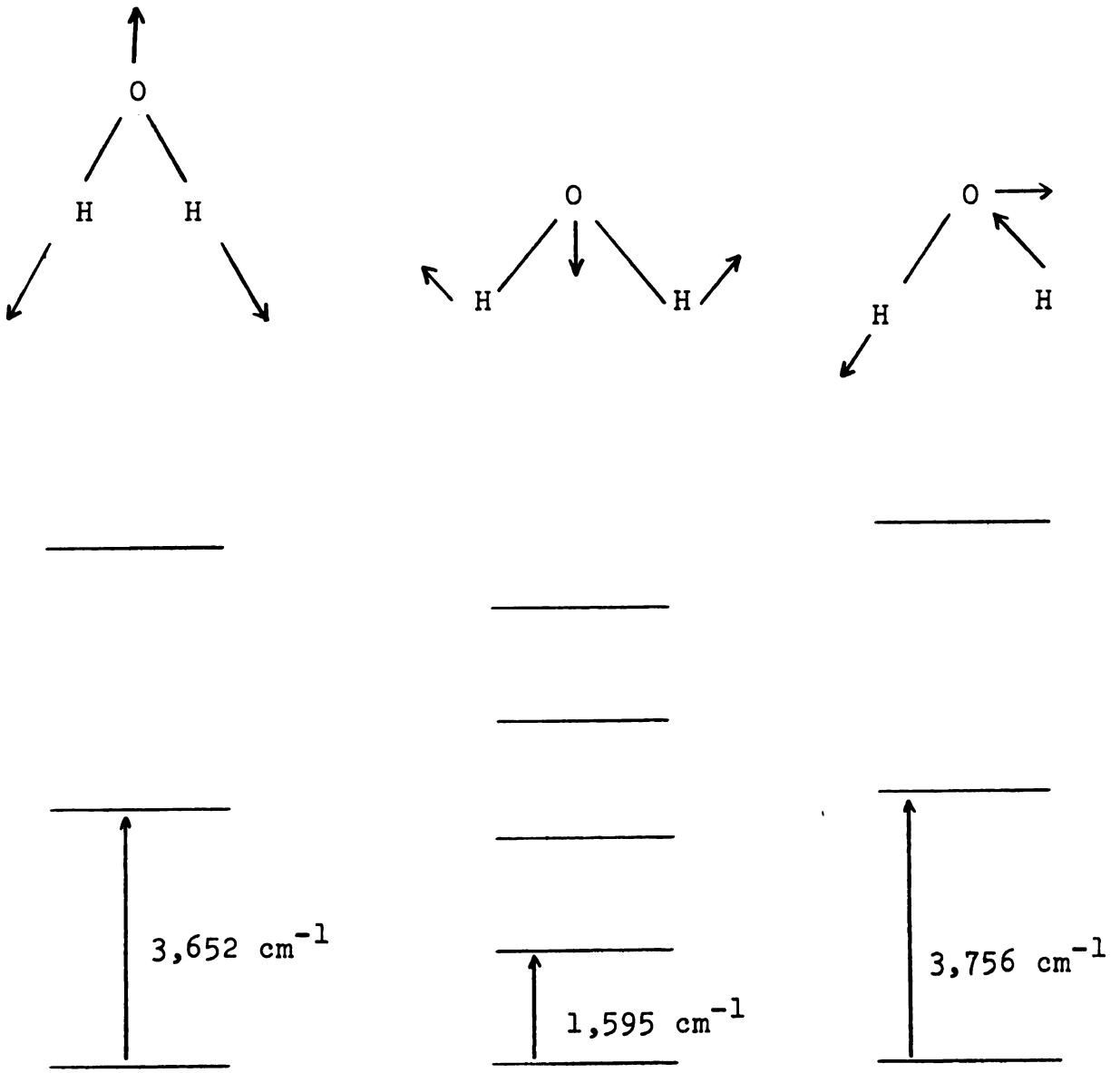

Fig. 2-5. Modes of vibration for water and associated energy levels.

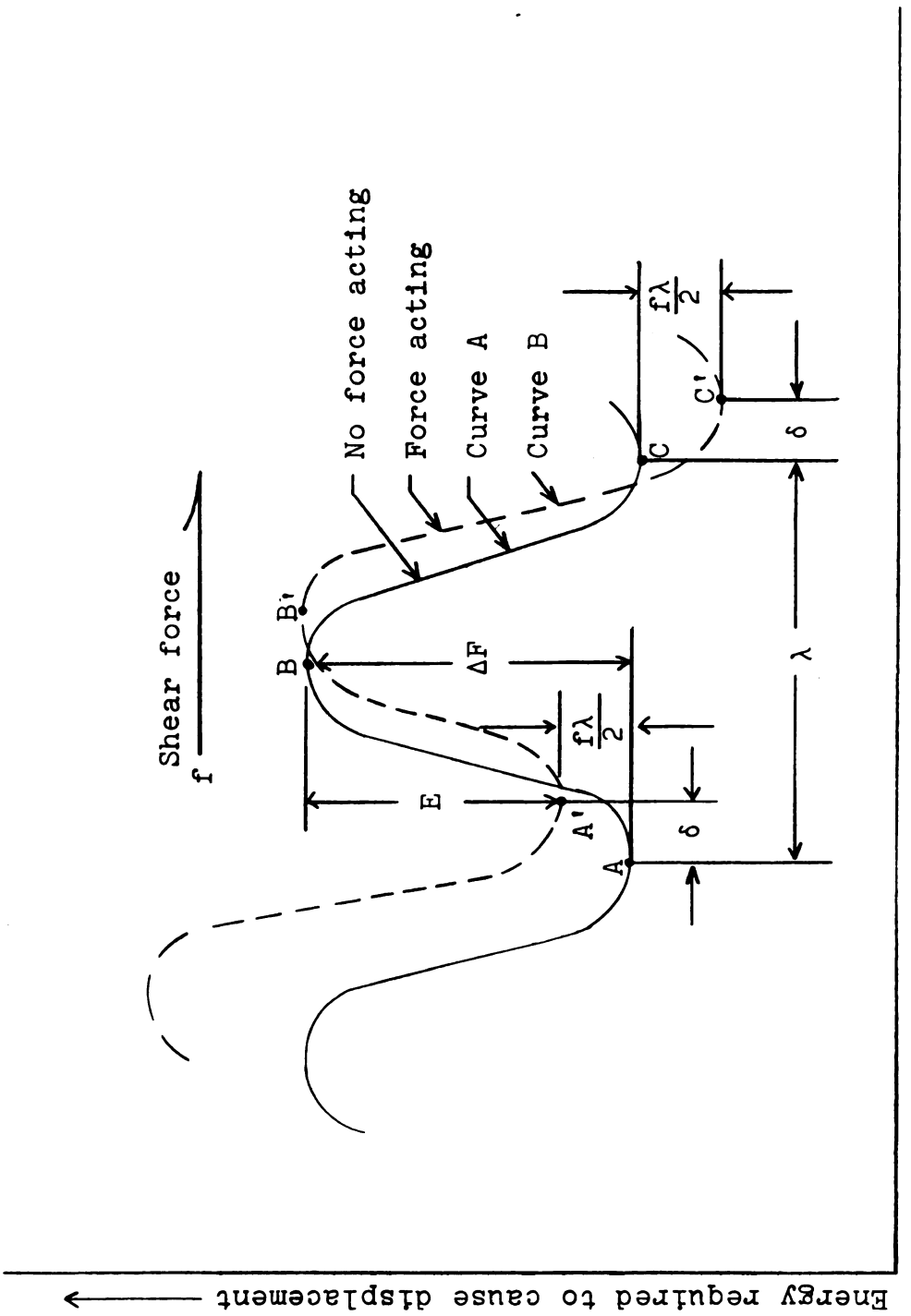

Fig. 2-6. Representation of energy barriers.

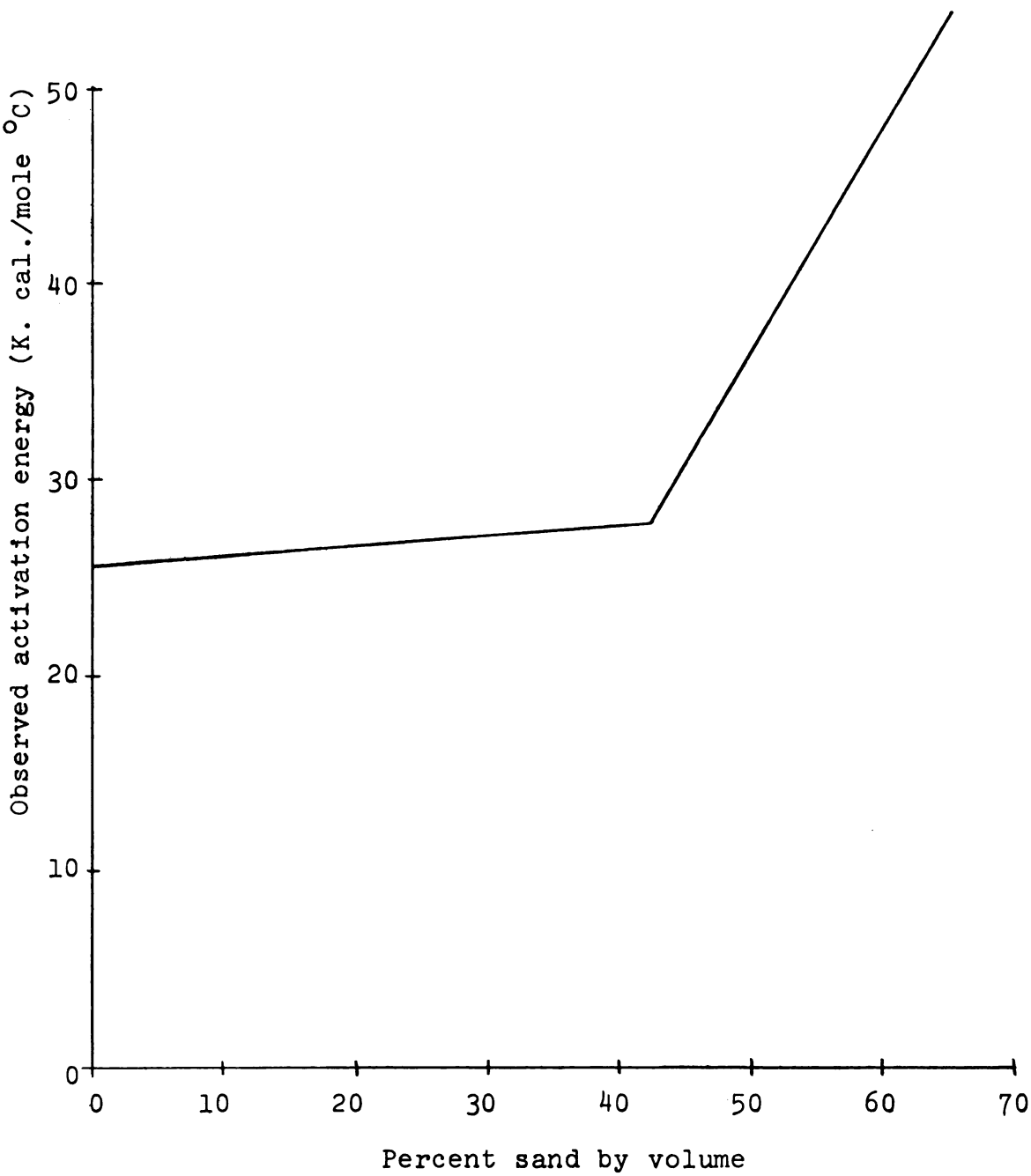

Fig. 2-7. Observed activation energy versus percent sand by volume (after Goughnour, 1967).

CHAPTER III

MATERIALS AND METHODS

The soil used in this investigation was a glacial lake clay from Sault Ste. Marie, Michigan. It is pedalogicly classified as Ontonogan and the basic properties are listed below. The grain size distribution curve is shown in Figure 3-1.

Index Properties

Properties	Per Cent or Number
Liquid Limit	60%
Plastic Limit	24%
Plasticity Index	36%
Specific Gravity	2.70
Less than 2μ	60%
Specific surface Area	290 sq. M./g/
Cation Exchange Capacity	28 meg/100 g.

Mineral Content of Fraction Less than 2μ

Illite	50%
Vermiculite	20%
Chlorite	15%
Kaolinite	5%
Quartz and Feldspar	10%

A quantity of the soil was treated with 1N hydrochloric acid to dissolve the carbonates and then washed with distilled water until the filtrate was free of chlorides as indicated by the silver nitrate test. It was then divided into three separate samples which were soaked in lithium, sodium or potassium chloride and again washed with distilled water and air dried.

In order to obtain further information on the role of the adsorption complex in the creep mechanism, a portion of each of the three samples was heated at 165°C. for seven days and then saturated with carbon tetrachloride. This procedure dehydrated the clay and caused the double layer to collapse. The non-polar carbon tetrachloride does not form an oriented adsorbed layer and the clay loses many of its common characteristics. For example, it becomes almost non-plastic.

Viscosity Tests

Viscosity measurements were made on the fluid soil-water mixtures with a "Brookfield" viscometer which operates on the principle of a rotating disc as illustrated in Figure 3-2. The calibration of the instrument was checked by using glycerin-water mixtures. The exact proportions of these mixtures were checked with a specific gravity hydrometer.

The soil-water mixtures were dispersed in a standard soil dispersion unit and allowed to stand for one hour

before testing. This permitted the coarser particles to settle out and eliminated the problem of rapidly changing density during the period of measurement. When the measurement was made, 25 ml. of the mixture was withdrawn from the vicinity of the disc and oven dried to determine the concentration of solids in grams per litre. All of the viscosity tests were performed in a thermostatically controlled water bath and the temperature of each mixture was checked before testing.

Creep Tests

Remoulded samples of each of the three soils were consolidated in triaxial compression cells at pressures of 1.75, 3.5 and 7.0 kg./sq. cm. then subjected to creep at constant volume by the application of axial loads. The initial axial stress for each of the consolidation pressures was 0.83, 1.25, and 1.66 kg./sq. cm. respectively. When secondary creep was established, an additional increment of axial stress equal to 0.104, 0.208 or 0.416 kg/sq. cm. was added. These axial stresses were applied by means of dead weights and the figures quoted are in terms of total stress. When secondary creep was again established, a further increment of the same magnitude was applied. The room temperature for those tests was controlled to 25°C ± 1°C.

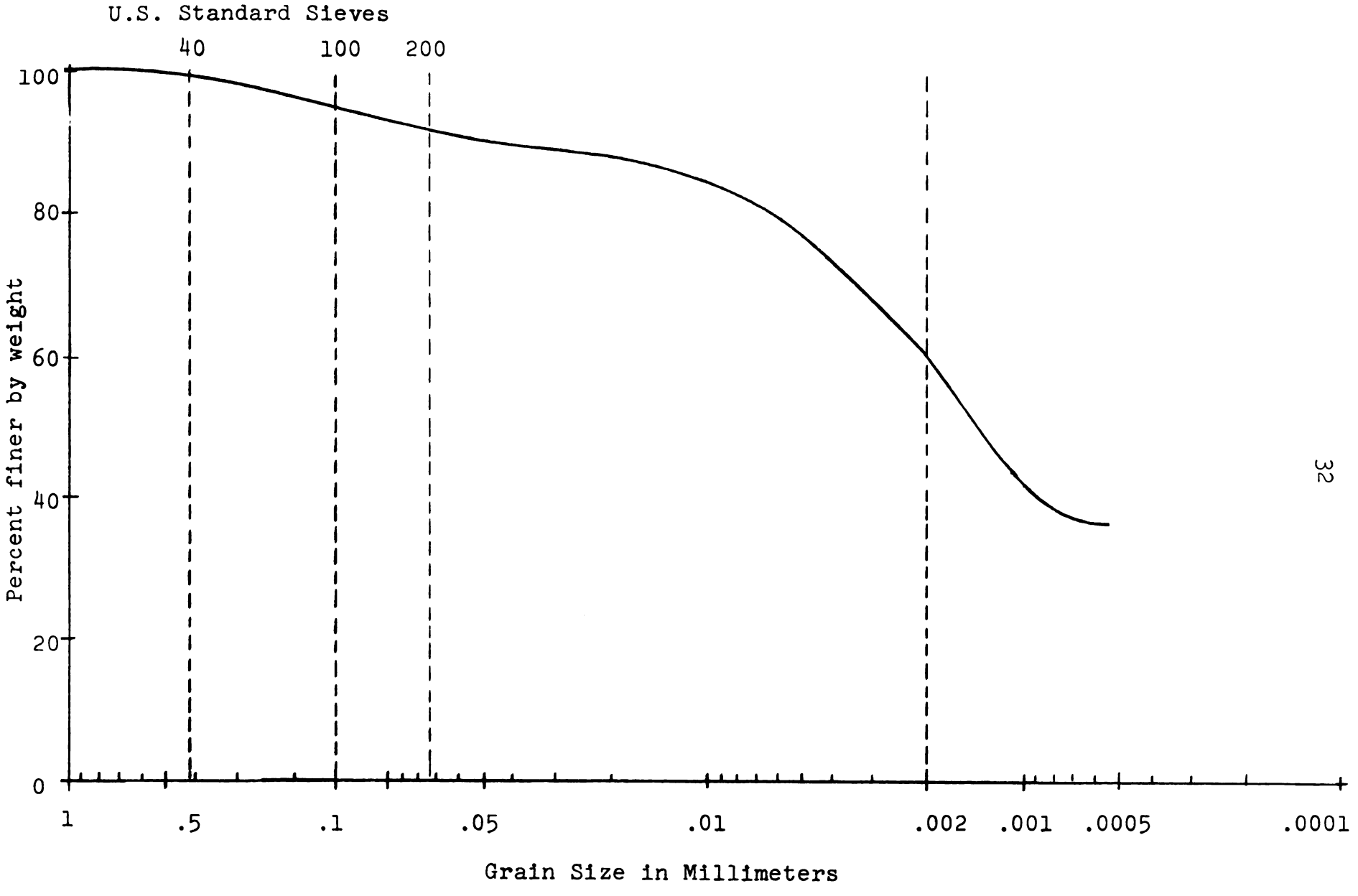

Fig. 3-1. Grain size distribution curve for Sault Ste. Marie Clay.

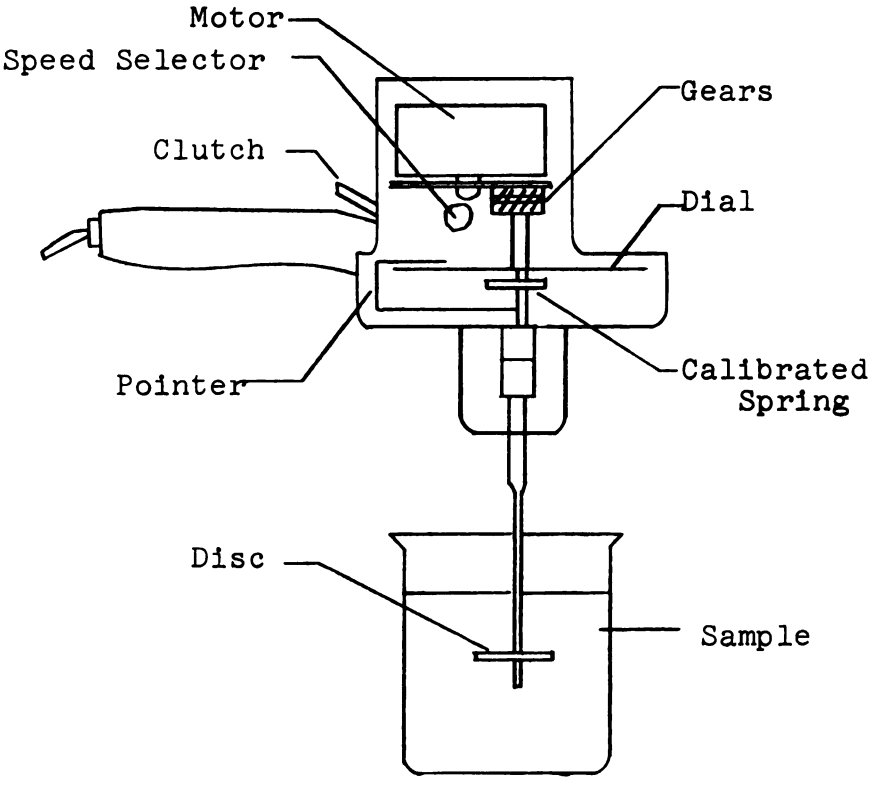

Fig. 3-2. Brookfield viscometer

CHAPTER IV

EXPERIMENTAL RESULTS

Viscosity Tests

Viscosity measurements were made over a range of soil concentrations for each of the lithium, sodium and potassium saturated soil samples at temperatures of 25, 35 and 45°C. As the concentration of soil solids was increased, the viscous flow changed from Newtonian to thixotropic. The limit for Newtonian flow of the lithium and sodium saturated samples was of the order of 100 g./litre, but for the potassium saturated sample it extended to about 500 g./litre. The variation in the coefficient of viscosity with concentration of soil solids for each of the three soils at 25°C is shown in Figure 4-1 and for the potassium saturated soil at each temperature in Figure 4-2.

Values of the free energy of activation ΔF were calculated by the use of equation (2-30) in the form

$$\ln \eta = \ln \frac{h}{V_f} + \frac{\Delta F}{R} \left(\frac{1}{T}\right) \qquad (4\text{-}1)$$

from which it is seen that there is a linear relationship between $\ln \eta$ and $(1/T)$. From Figures (4-3), (4-4) and (4-5) this is found to be approximately true for each soil

and the slope of the lines is parallel to the line for pure water. The approximation is due to straight lines being drawn through the points recognizing that ΔF for water is also a function of temperature. This variation is not significant over the temperature range considered and the value of ΔF may be taken as 3.8 k. calories/mole. Thus there is no evidence that ΔF varies with concentration of soil solids over the range of Newtonian flow. There is a change in the size of the flow units with concentration and this is shown in Figure (4-6).

Creep Tests

The results of a typical triaxial creep test are illustrated in Figure (4-7) which shows the variation of natural strain with time and the effect of the additional increments of axial stress. All of the samples gave curves of similar form. At low stress levels there is a simple linear relationship between the strain and the logarithm of the time but as the stress level is increased there is a pronounced deviation from such a relationship. This point has been discussed by Singh and Mitchell [1968]. A linear relationship was observed between the logarithm of the strain rate and the strain which was found to be useful in the evaluation of the activation energies.

From equation (2-31),

$$\ell n\ \dot{\gamma} = \ell n\ kT/h - \Delta F/RT + \tau\ V_f/2kT \qquad (4\text{-}2)$$

and if $\dot{\gamma}$ is changed by the application of an additional increment of stress,

$$\ell n\ (\dot{\gamma}_1/\dot{\gamma}_2) = (\tau_1 - \tau_2)\ \ V_f/2kT \qquad (4\text{-}3)$$

Since $\dot{\gamma}$ is not constant, possibly due to continuous structural changes as the creep proceeds, it is necessary to determine $\dot{\gamma}_1$ and $\dot{\gamma}_2$ at the same instant. This was accomplished by calculating $\dot{\gamma}_1$ and $\dot{\gamma}_2$ at each side of the discontinuity caused by application of the additional stress increment. The application of additional stress causes rapid initial strain due to elastic compression of the system and a certain amount of additional primary creep. It is therefore necessary to make use of the linear relationship which exists between the logarithm of the strain rate and the strain to extrapolate back to the initial value as illustrated in Figure (4-8). The usual assumption that the intensity of plastic action is governed by the octahedral shear stress is also made here and octahedral shear stresses are employed in all relevant equations.

$V_f/2kT$ was calculated by means of equation (4-3) from the data in Figure (4-8) and then ΔF was calculated from equation (4-2) as illustrated in the example below. The results are listed in Table (4-1).

Example

Potassium saturated sample, σ_3 = 3.5 kg./sq. cm. initial axial stress = 1.25 kg./sq. cm., first increment of axial stress of 0.208 kg./sq. cm., temperature 298°K., Boltzmann's constant k = 1.380×10^{-16} erg/degree molecule, Planck's constant h = 6.624×10^{-27} erg-sec and the gas constant R = 1.987 calories/degree mole. From equation (4-3)

$$V_f/2kT = \ell n\ (\dot{\gamma}_1/\dot{\gamma}_2)/(\tau_1 - \tau_2)$$

From Figure (4-8)

$$\dot{\gamma}_1 = 125 \times 10^{-6} \text{ and } \dot{\gamma}_2 = 8.4 \times 10^{-6}$$

hence

$$\ell n\ (\dot{\gamma}_1/\dot{\gamma}_2) = 2.698$$

Now τ_1 and τ_2 are octahedral shear stresses and since

$$\tau_{oct} = \frac{\sqrt{2}}{3}\ (\sigma_1 - \sigma_3)$$

$$\tau_1 - \tau_2 = \sqrt{2/3}\ \text{(axial stress increment)}$$

$$= 0.098 \text{ kg./sq. cm.}$$

therefore

$$V_f/2kT = 2.698/0.098$$

$$= 27.50 \text{ sq. cm./kg.}$$

$$= 27.00 \times 10^{-6} \text{ sq. cm./dyne.}$$

so that

$$V_f = 27.00 \times 10^{-6} \times 2 \times 1.38 \times 10^{-16} \times 298$$

$$= 2.25 \times 10^{-18} \text{ c.c.}$$

From equation (4-2)

$$\Delta F = RT \ln (kT/h) + \tau RT (V_f/2kT) - RT \ln \dot{\gamma}$$

In Figure (4-8) the strain rate is shown in terms of axial strain for convenience, but for this calculation it must be in terms of octahedral shear strain which means that the axial strain rate figure must be multiplied by $\sqrt{2}$. Also h should be multiplied by 60 to convert to erg. minutes.

Now considering the end of the first period of creep when the axial stress was 1.25 kg./sq. cm.

$$\Delta F = 15{,}130 + \sqrt{2}/3 \times 1.25 \times 981 \times 10^3 \times 1.987 \times 298 \ (27 \times 10^{-6}) - 1.987 \times 298 \ (-11.33)$$

$$= 31.4 \text{ k. calories/mole.}$$

TABLE 4.1.--Values of Activation Energy and Flow Volume from Creep Tests.

Soil Treatment	Consol. Pressure kg./cm.^{2}	Dry Density g./c.c.	Initial Axial Stress kg./cm.^{2}	First Axial Stress Increment			Second Axial Stress Increment		
				kg./cm.^{2}	V_f $\mathring{A}^3 \times 10^6$	ΔF k. cal./mole	kg./cm.^{2}	V_f $\mathring{A}^3 \times 10^6$	ΔF k. cal./mole
Lithium	1.75	1.55	0.83	0.104	2.1	26.4	0.104	1.5	25.8
	3.50	1.70	1.25	0.208	1.7	28.3	0.208	1.4	28.2
	7.00	1.88	1.66	0.416	1.2	27.8	0.416	1.5	32.0
Sodium	1.75	1.53	0.83	0.104	3.0	29.0	0.104	3.0	30.2
	3.50	1.72	1.25	0.208	1.7	28.4	0.208	2.0	30.6
	7.00	1.88	1.66	0.416	0.7	25.0	0.416	1.2	27.0
Potassium	1.75	1.58	0.83	0.104	3.8	31.6	0.104	4.2	34.9
	3.50	1.72	1.25	0.208	2.3	31.4	0.208	2.3	33.1
	7.00	1.87	1.66	0.416	1.6	30.2	0416	2.0	35.4
Lithium CCl_4	1.74	1.62	0.83	0.104	1.1	24.1	0.104	1.7	26.3
	3.50	1.74	1.25	0.208	1.2	26.0	0.208	1.1	26.6
	7.00	1.95	1.66	0.416	0.6	24.2	0.416	0.7	25.6
Sodium CCl_4	1.75	1.60	0.83	0.104	1.5	24.6	0.104	1.6	26.3
	3.50	1.74	1.25	0.208	1.1	25.7	0.208	1.4	28.0
	7.00	1.92	1.66	0.416	0.8	25.5	0.416	0.7	26.0
Potassium CCl_4	1.75	1.63	0.83	0.104	8.6	47.1	0.104	2.8	31.0
	3.50	1.76	1.25	0.208	1.5	28.1	0.208	1.5	29.1
	7.00	1.93	1.66	0.416	1.0	27.3	0.416	0.8	27.9

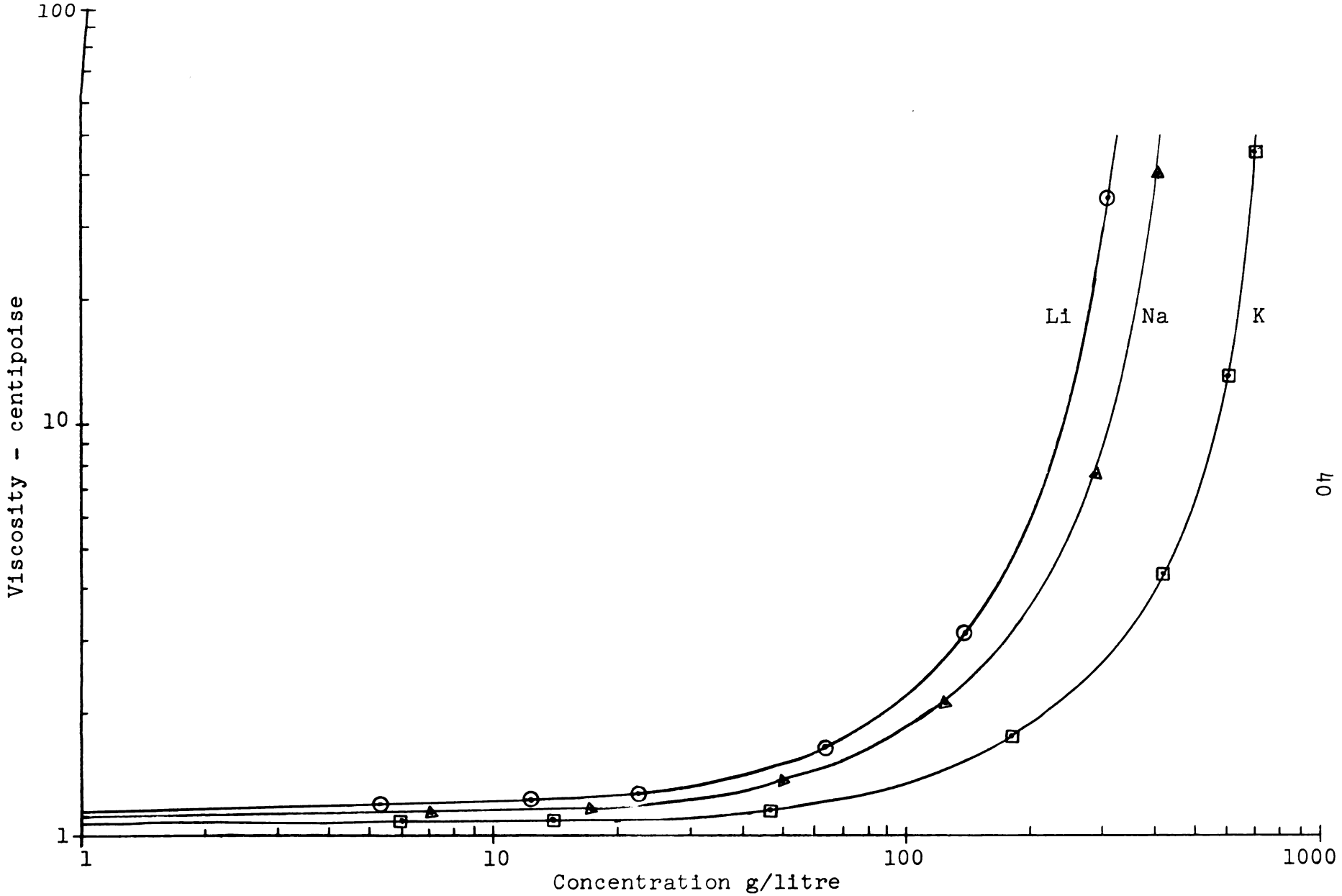

Fig. 4-1. Viscosity of soil-water mixtures at 25° C.

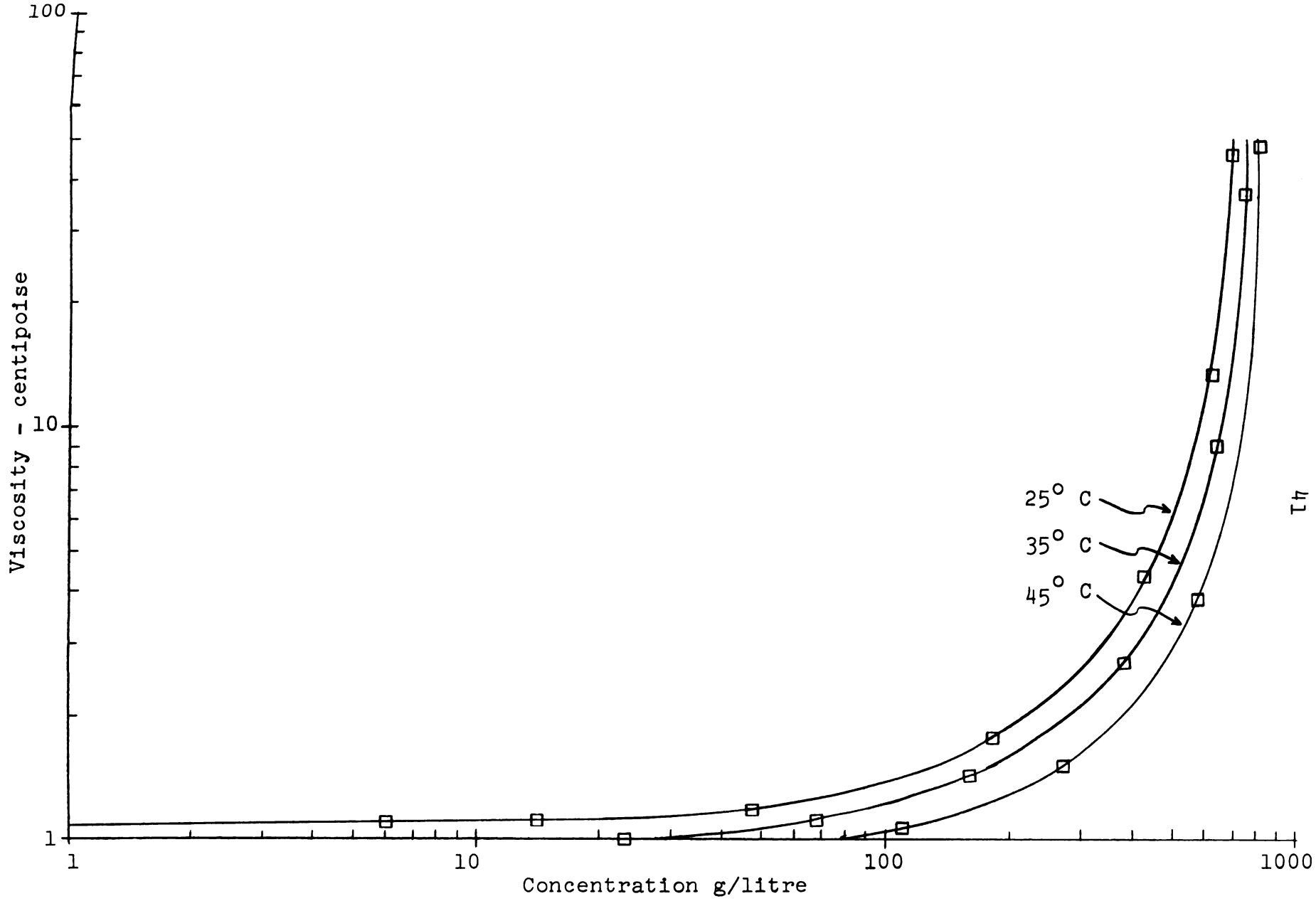

Fig. 4-2. Variation of viscosity with concentration at different temperatures for potassium saturated clay.

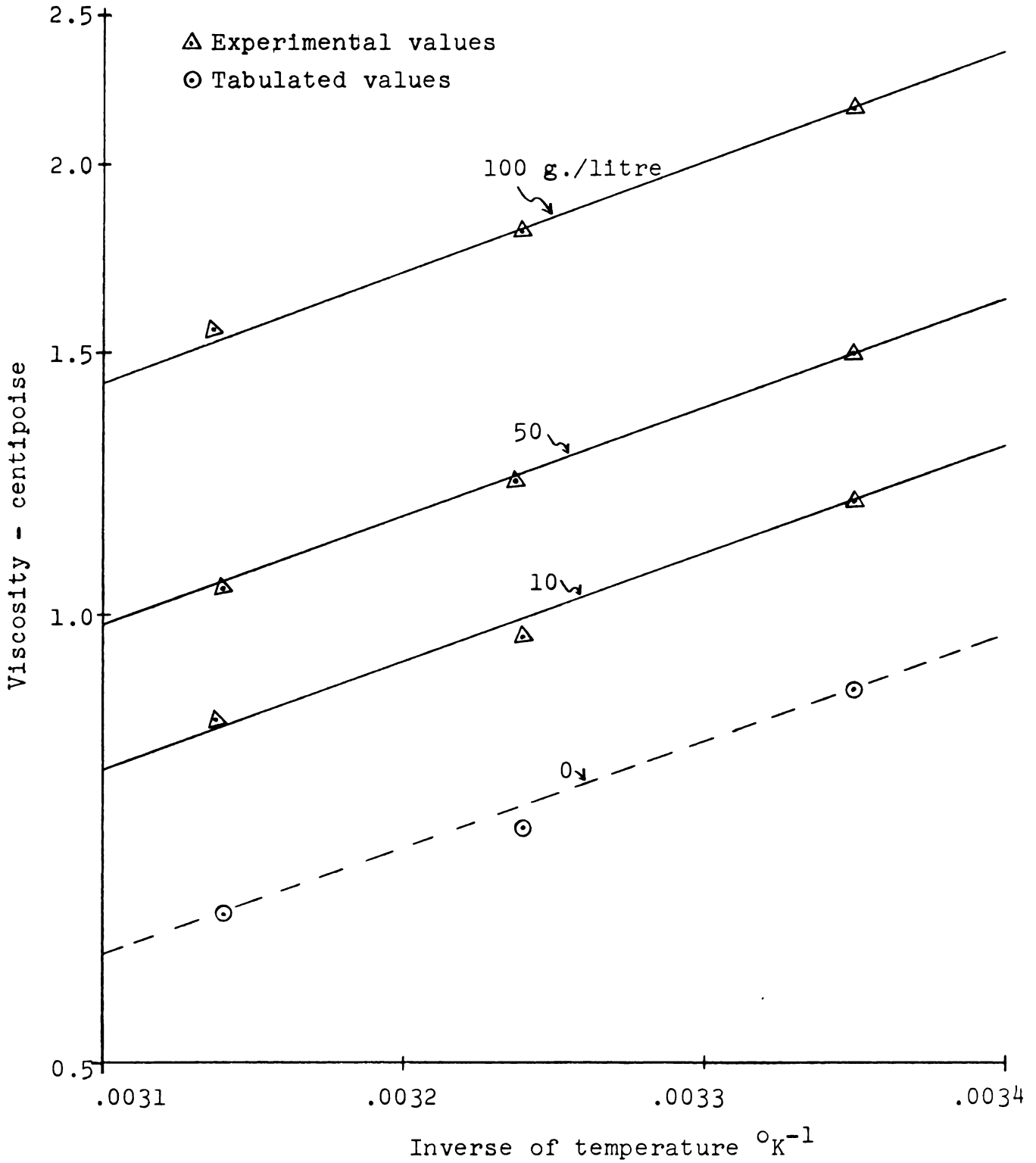

Fig. 4-3. Variation of viscosity with temperature for lithium saturated clay.

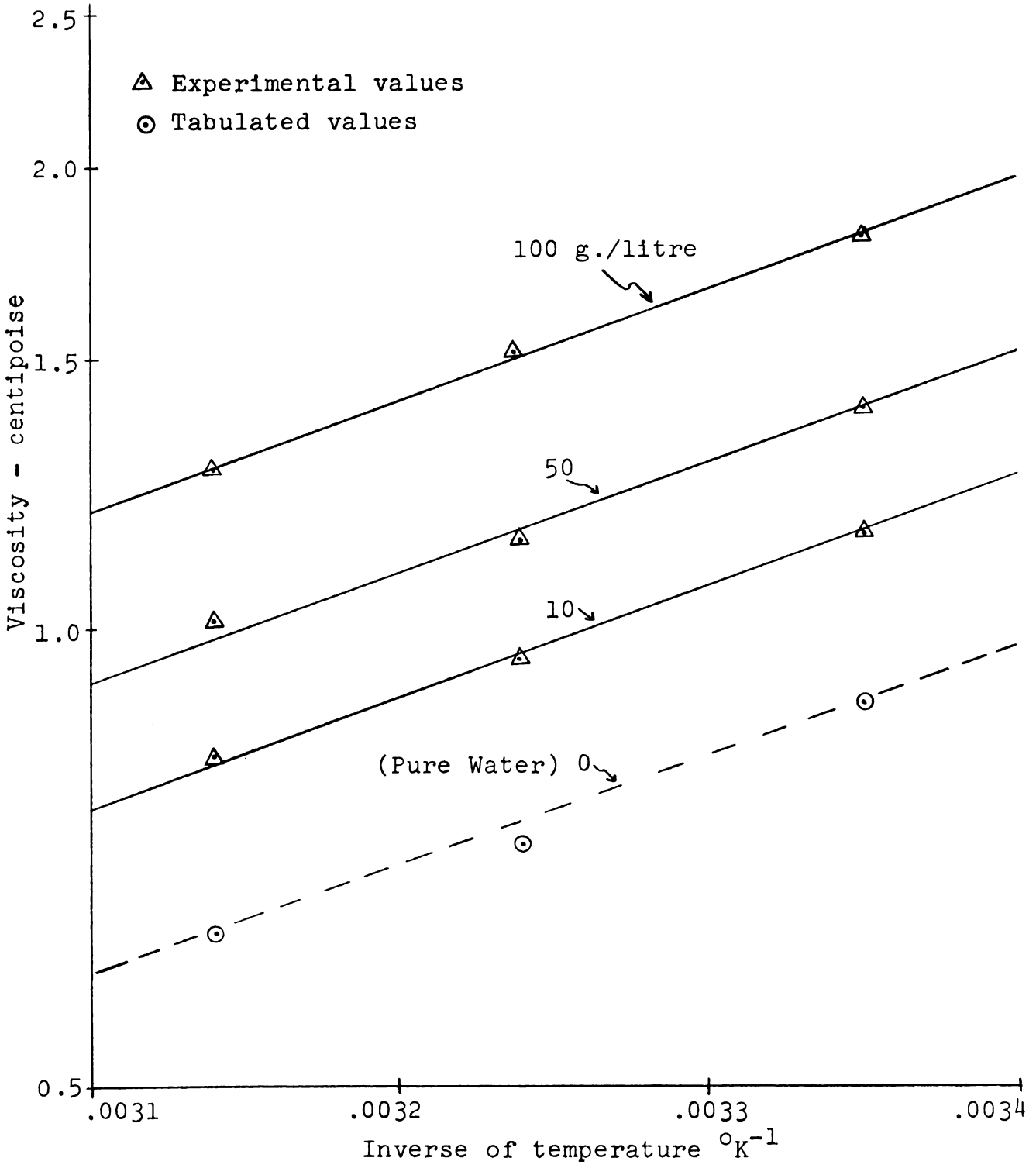

Fig. 4-4. Variation of viscosity with temperature for sodium saturated clay.

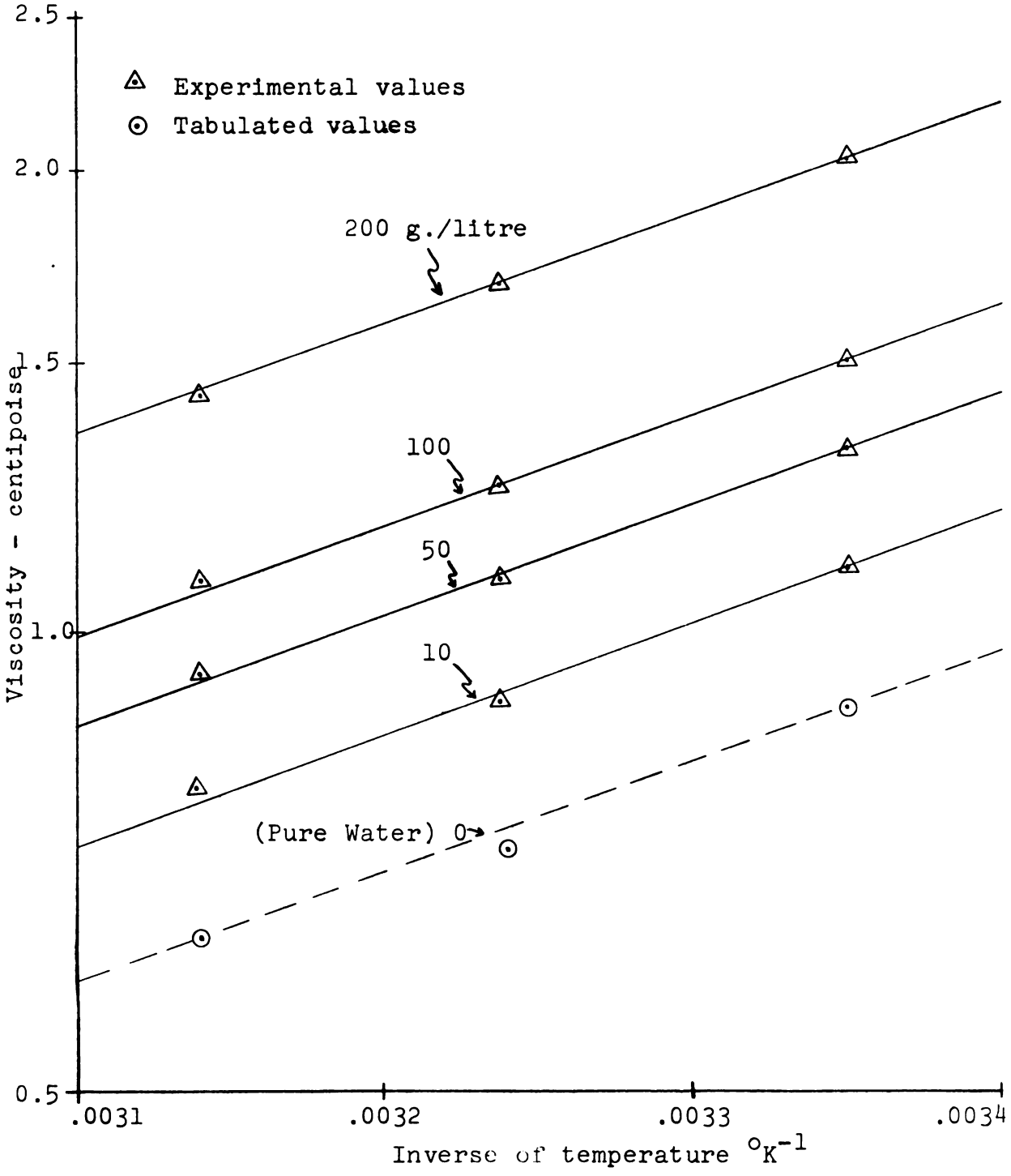

Fig. 4-5. Variation of viscosity with temperature for potassium saturated clay.

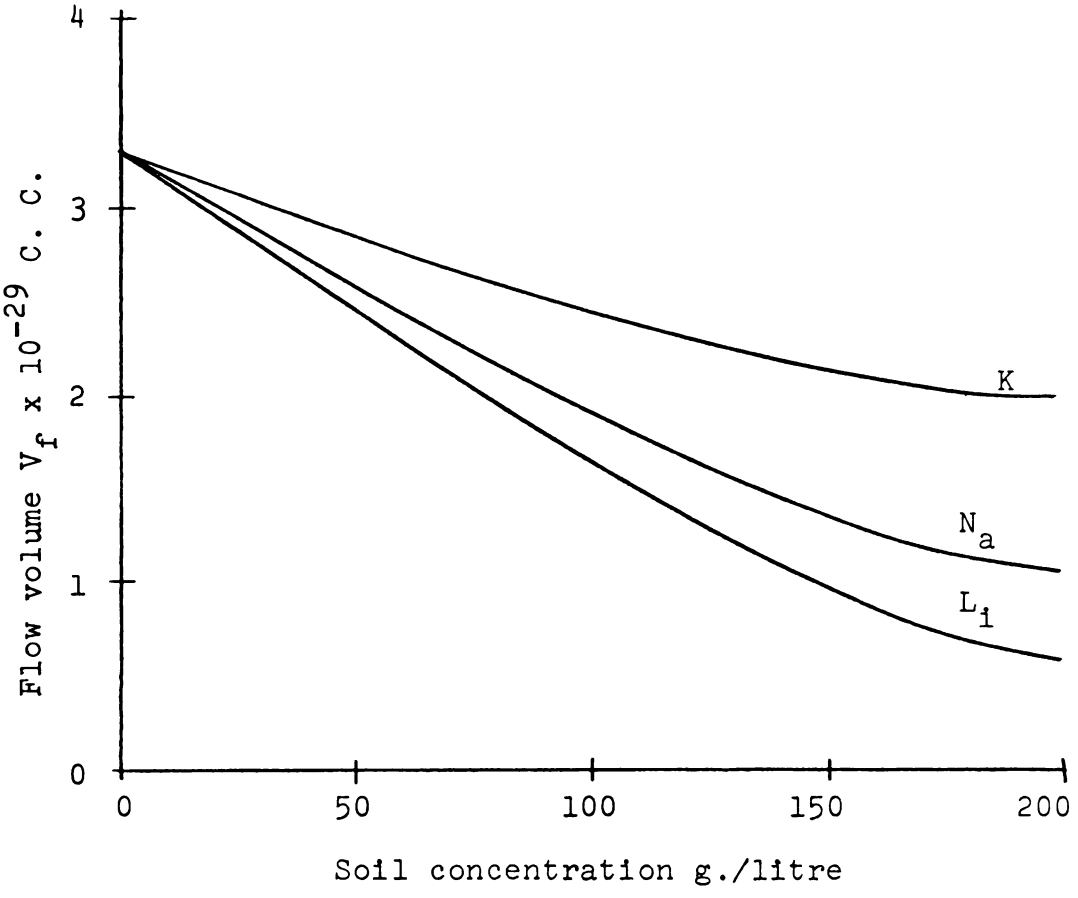

Fig. 4-6. Variation of flow volume with concentration of soil.

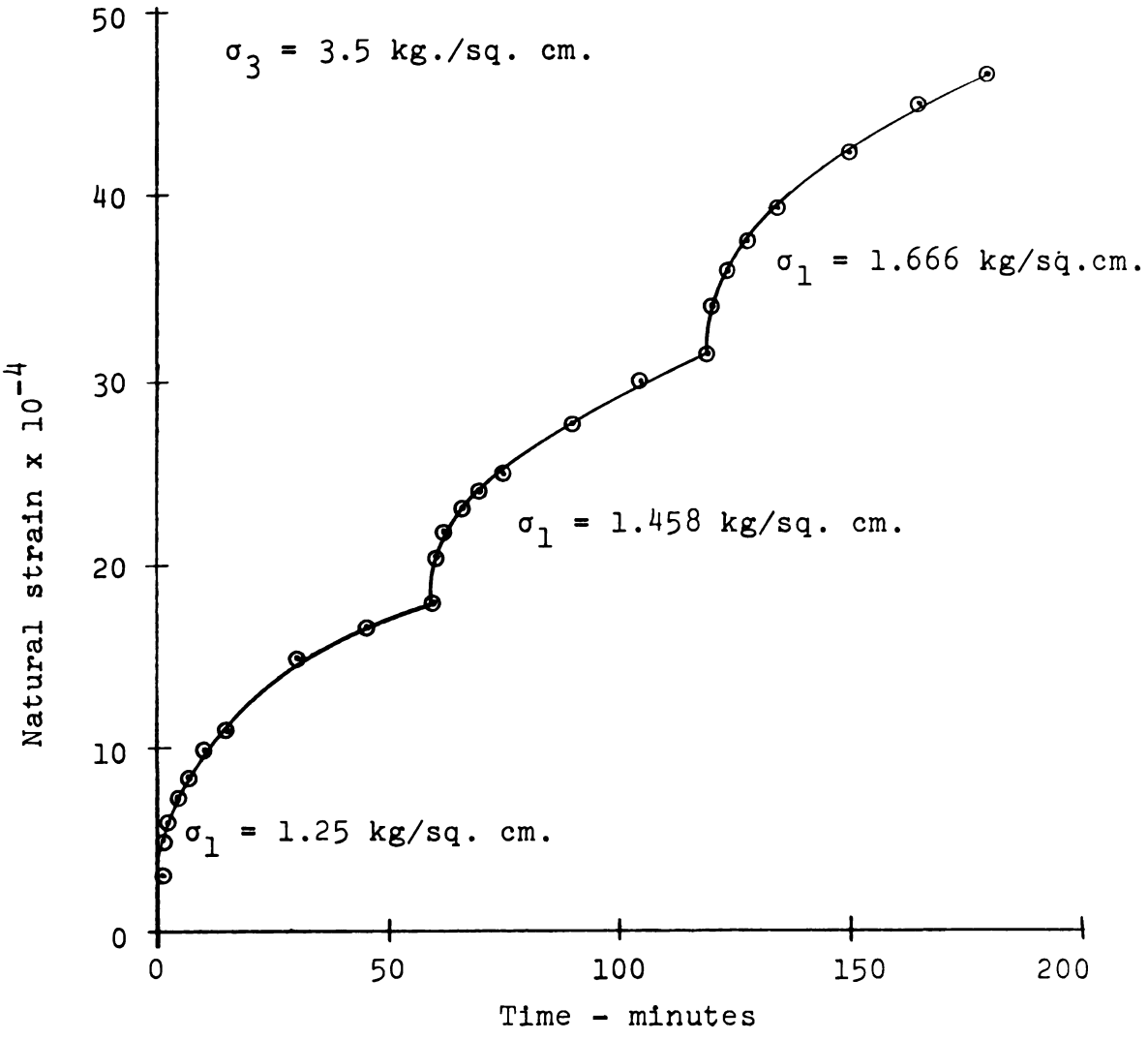

Fig. 4-7. Creep curve for potassium saturated clay.

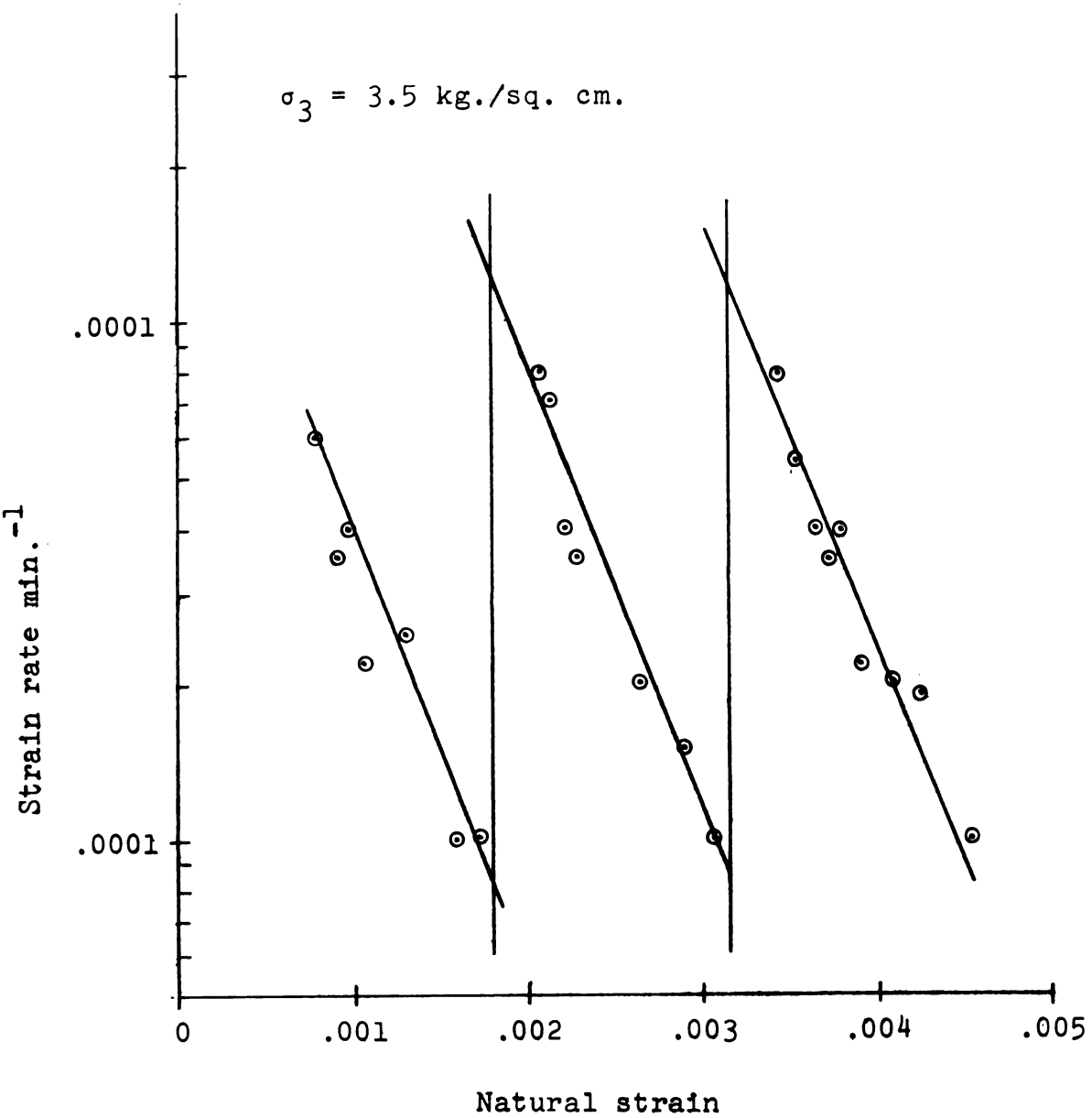

Fig. 4-8. Variation of strain rate with strain for potassium saturated clay.

CHAPTER V

ANALYSIS AND INTERPRETATION

Theory

If the values of ΔF are to be regarded as other than merely parameters in the Arrhenius equation, and they are to be given a physical interpretation with respect to the nature of the rate controlling bonds, further consideration must be given to the assumptions which are implicit in the derivation of the rate equation.

Up to this point it has been assumed that the flow process involves the movement of a particle by a single step from an equilibrium position A to the next equilibrium position B. It may be necessary for the particle to move through a series of intermediate steps before reaching position B and then the strain rate is given by:

$$\dot{\gamma} = \frac{\Delta\gamma}{t_1 + t_2 + \cdots + t_n} \qquad (5\text{-}1)$$

where t_n is the delay time associated with each obstacle. Equation (5-1) may be written as

$$\dot{\gamma} = \frac{\Delta\gamma}{A_1 \exp.\ (\Delta F_1/RT) + \cdots + A_n \exp\ (\Delta F_2/RT)} \qquad (5\text{-}2)$$

where A_n are constants with other symbols as previously defined. It is seen from these equations that if one step is much slower than any of the others, then it may be regarded as the rate-controlling step and that it is associated with the highest energy barrier. In this case the other steps may be neglected. If two or more steps are of the same order of magnitude the calculated value of ΔF will have no meaning unless it can be resolved into its component parts.

There may also be more than one available path by which the particles may proceed so that several different mechanisms are operating in parallel. In this case the strain rate is given by

$$\dot{\gamma} = \dot{\gamma}_1 + \dot{\gamma}_2 + \cdots \dot{\gamma}_n \qquad (5\text{-}3)$$

or

$$\dot{\gamma} = A_1 \exp. (-\Delta F_1/RT) + A_2 \exp (-\Delta F_2/RT) + \cdots \qquad (5\text{-}4)$$

The rate-controlling step will now be the fastest one, but again, if two or more steps are of the same order of magnitude as the fastest step, the calculated value of ΔF will have no physical meaning.

Some of the possible mechanisms which could be operating simultaneously in the ice and soil water systems to be considered are:

(i) the flow of free water

(ii) the creep of polycrystalline ice

(iii) the relative movement of soil grains, which may involve the action of adsorbed water.

These three systems will now be considered before attempting to analyze the various combinations of them.

The Flow of Free Water

In this context, "free water" refers to water which is not under the action of surface forces from the clay particles. However, there is a mutual association between the individual water molecules in the form of hydrogen bonding. This is best described by reference to the structure of ice shown in Figure (5-1) in which the hydrogen bonding is complete and each hydrogen atom shares its electron with two oxygen atoms to make a regular hexagonal crystal arrangement. In the liquid phase, some of these bonds are destroyed and individual molecules may exist. It is thought that the closer packing of these free molecules contributes to the fact that the density of water is greater than that of ice. As the temperature is increased the thermal energy of the molecules increases and progressively more of the hydrogen bonds are broken as indicated in Table (5-1).

In order for a molecule to move into a new position, a hole must be available for it. The free energy of activation of viscous flow therefore generally consists of

TABLE 5-1.--Degree of Hydrogen Bonding of Water.

Temperature	State	Degree of Bonding
0° C	Ice	100%
0° C	Water	85%
40° C	Water	50%
100° C	Steam	10%

two parts, (a) the energy required to form the hole and (b) the energy required for the molecule to move into the hole. Now it may be shown that the energy required to form a hole in a liquid of molecular size is equal to the energy required to evaporate a molecule without leaving a hole. Since the necessary holes already exist in a liquid, the energy required to form the hole will only be that which is necessary to increase an existing hole to molecular size. This is a relatively constant fraction of the energy of vaporization. In non-associated liquids, a plot of viscosity against 1/T will give a linear relationship, but in the case of water the plot is slightly curved. This curvature is due to the fact that the free energy of activation of flow consists not only of the energy required to form a hole, but also the energy required to break the hydrogen bonds with which it is tied to its neighbors. As the temperature is increased, the number of bonds decreases. The free energy of activation for viscous flow of water is

about 4 k. calories/mole and the strength of a hydrogen bond is about 6 k. calories/mole [Glasstone, 1959].

Significant changes in ΔF with pressure only occur with pressures of the order of thousands of atmospheres and hence are not directly relevant here. The principle which is involved will be relevant in later discussion. If the external pressure on the system is increased, the formation of a hole will involve doing work against this pressure. Hence ΔF will be increased by an amount $p\Delta V$.

The Creep of Polycrystalline Ice

Values quoted in the literature for the activation energy of polycrystalline ice range from 10.7 k. calories/mole [Mellor and Smith, 1967] to approximately 25 k. calories/mole [Dillon and Andersland, 1967] with small variations in this latter value according to the temperature and pressure. There is some confusion in terminology which accounts for most of the apparent differences. Many of the authors, including Mellor and Smith, have determined the enthalpy of activation (ΔH) and referred to it as the free energy of activation. According to Dillon and Andersland [1967], the value of ΔH is 11.4 k. calories/mole which is the order of the commonly quoted values.

The number of bonds which must be broken to permit slip along the basal plane of ice is much less than the number which must be broken for slip to occur normal to

this plane. Consequently all reported observations of the creep of a single ice crystal indicate that the creep mechanism is associated with movement along the basal plane. In the polycrystalline state where the crystals are randomly oriented this movement is restricted at the grain boundries, and the additional mechanisms which come into operation include cavity formation, accommodation cracking, rotation and migration of the grain boundaries [Gold, 1963].

The Relative Movement of Soil Grains

If the creep of soil is a thermally activated process, then some form of molecular bonding must exist between the grains. This may be in the form of hydrogen bonding through the adsorbed water layer or it may be in the form of ionic bonding as the result of direct mineral to mineral contact. The probability that any such mechanism exists will be discussed later in this chapter on the basis of the experimental values obtained for the free energy of activation. There is one other factor contributing to the experimental value of ΔF which must be considered, and that is the energy involved in the creep of a frictionless unbonded soil.

The stress required to induce flow in a closely packed hexagonal arrangement of spherical balls was considered by Thurston and Deresiewicz [1959]. Any one ball in such an arrangement rests on three balls in the layer

below, makes contact with six others in the plane of its centre, and is acted upon by three contact forces normal to its surface from the three balls in the layer above. The force acting on the sphere in the direction normal to the hexagonal layer is the resultant of each of these three normal stresses which have a magnitude of $\sqrt{2}\ R^2\ \sigma_3$ where σ_3 is the hydrostatic pressure acting on the system and R is the radius of the balls. Each of these forces has a direction cosine with the vertical of $\sqrt{2}/\sqrt{3}$. The resultant force normal to the layer is therefore $2\sqrt{3}\ R^2\ \sigma_3$.

If a force L is now applied at angles α and β to the z and y axes, where z is normal to the plane of the hexagon, so that L has both shear and normal components, it can then be shown that the ratio of the shearing to the normal forces is given by:

$$\frac{L \cos \beta}{2\sqrt{3}\ R^2\ \sigma_3 + L \cos \alpha} = \frac{\sqrt{3}}{2\sqrt{6}} = 0.35 \qquad (5\text{-}5)$$

if the coefficient of friction of the material is zero. The existence of a normal force on the plane of sliding will therefore mean that some of the applied shear stress will be utilized in moving the soil grains even if there is no form of bonding between them. The stress required to overcome this resistance on the octahedral plane will be $0.35 \times 1/3\ (\sigma_1 + \sigma_2 + \sigma_3)$ and therefore equations (2-29), (2-29a) and (2-31) should be modified to read

$$\dot{\gamma} = \frac{2kT}{h} \exp. (-\Delta F/RT) \sinh ((\tau - 0.35\sigma_{oct.}) V_f/2kT) \quad (5\text{-}6)$$

$$\dot{\gamma} = (\tau - 0.35\sigma_{oct.}) V_{f/h} \exp. (-\Delta F/RT) \quad (5\text{-}7)$$

and

$$\dot{\gamma} = \frac{kT}{h} \exp. (-\Delta F/RT) \exp. ((\tau - 0.35\sigma_{oct.})V_f/2kT) \quad (5\text{-}8)$$

The factor 0.35 may vary with the shape of the grains and the density of packing. Al-Nouri [1969] has shown experimentally that creep rates for frozen saturated sand decrease with increase in $\sigma_{oct.}$ while holding the deviatoric stress constant.

Soil Suspensions

The viscosity of the soil suspensions increased with increasing concentration of solids in the order Li, Na, K but no variation in the free energy of activation of flow was observed. In dilute suspensions where it is assumed that the grains are widely spaced, the flow mechanism is that of pure water with boundary conditions defined by the container and the soil grains. The effect of the adsorbed water layer on the grains is not fundamentally different from that of the boundary layer on the walls of the container.

The measurement of a coefficient of viscosity of a suspension has a real significance for such problems as the pumping of such a material, but for a fundamental investigation of the nature of the properties of the water and soil it may be preferable to regard such a measurement as the determination of the viscosity of water in a viscometer of complex boundary conditions and the Einstein equation (2-1) might be better written as

$$\eta_o = \eta/(1 + a\phi) \qquad (5\text{-}9)$$

and the results used to deduce facts about the nature of the boundary conditions. For example, the order of viscosities at a given concentration for each of the three samples tested would indicate that the effective volume of the lithium saturated clay was greater than that of the sodium saturated which was greater than that of the potassium saturated and due to the different degrees of hydration of their ions.

When the concentration is increased to the point that the particles come within range of their mutual force fields a multiple flow situation is established. The free water still follows its normal flow mechanism within the new boundary conditions but there is now the added flow mechanism of the interacting grains. The two systems can not be regarded as operating independently, for the rate of movement of the grains is controlled not only by the

activation barriers of the inter-particle bonds but also by the viscous drag of the water. When a bond is broken, the movement to the new equilibrium position is restrained by the effect of the water thus establishing the time delay associated with thixotropic materials of this type. Hence an activation energy determined from the bulk behavior would represent some combinations of the various energies involved.

It may therefore be concluded that the calculated values of the activation energy for each of the samples is valid since the method of calculation involves a ratio of viscosities and the measured viscosity differs from that of water by a constant factor which will cancel out. The calculation of the flow volume involves the direct use of the measured viscosity and will therefore deviate from the true value in inverse proportion to this factor.

Unfrozen Soil

The modified strain rate equation (5-6) implies the existence of a yield stress, below which creep will not occur. This phenomenon is known to occur in sands but does not exist in saturated clays. Even a small stress will produce creep at the correspondingly slow rate. The experimental values of ΔF listed in Table (4-1) may therefore be accepted without modification.

It is significant that there is no apparent difference between the values of ΔF for any of the three soils

even when dehydrated and mixed with carbon tetrachloride. This would appear to eliminate any possibility that the source of the bonding is associated with the adsorption complex. In addition, the mean value of approximately 28 k. calories/mole is within the range of ionic and covalent bonding and is five times the strength of a hydrogen bond. It might be thought that value of 28 is suggestive of the 25 k. calories/mole that Dillon and Andersland [1967] found for polycrystalline ice and it could be postulated that the bonding was associated with the first one or two molecular layers of adsorbed water where the structure is ice-like. The lack of variation in the values obtained from the carbon tetrachloride samples precludes such a possibility. The only bonding mechanism which can be consistent with the data is that of a portion of the edge of a clay plate which is deficient in oxygen (or hydroxyl) atoms and has a local positive charge, associates with a portion of another plate which has lost a metallic atom and has a local negative charge. A junction would then be formed between the two plates, but due to the lack of orientation would not be of full strength and would be readily broken.

The values of V_f also show no significant variation between the samples which lends support to the suggestion that the type of bond is similar in each case. While V_f is called the "flow volume," this is only true if the

stress on the flowing unit is equal to the applied stress. In the case of a particulate media where the spacing of the units is large in comparison to their size, a correction must be made in order to determine the actual volume of the flowing unit. If V_f is multiplied by the number of contacts per sq. cm., the length λ will be obtained and in the derivation it was assumed that all of the dimensions of the unit are of the same order of magnitude so that an approximation to the actual flow volume is given by λ^3.

The average volume of a particle of this clay has been estimated by Christensen and Wu [1964] to be 2×10^{-15} c.c. and from Figure (3-1) it is seen that 60% of the soil is less than 2 μ. Also from Table (4-1) the mean dry density of the samples is 1.75 g./c.c. The volume of clay per c.c. of soil is therefore 0.39 c.c. and the number of clay particles is approximately 2×10^{14}. Rosenquist [1959] has estimated that each particle forms six contacts, so that if this estimate is accepted, the number of contacts per c.c. will be three times the number of particles (since each contact is formed between two particles). The number of contacts per sq. cm. is then $(3 \times \text{no. of particles})^{2/3}$ which is 7×10^9. Hence the length λ is 1.2 $\mathring{A}$ and the actual flow volume is 1.7 $\mathring{A}^3$. This estimate of λ is approximately half of that which would be expected from the crystal structure of the

minerals. This discrepancy is probably related to the assumption that the shape of the flow unit was cubic, for while the dimensions of the unit would be of the same order of magnitude, they are unlikely to be equal. It is therefore considered to be a good estimate and does establish that the flow units involved are of molecular size. It is also observed that for each sample the value of V_f decreases with increasing density. This is to be expected as the contacts between the grains are improved.

Frozen Soil

The behavior of frozen soil is in many ways similar to that of soil suspensions. Goughnour [1967] has reported that at low concentrations there is a linear relationship between the creep rate and the volume of solids and an equation similar to the Einstein equation (2-1) could be proposed. A small increase in activation energy is reported over this range possibly due to the interlocking effect of the grains on the dislocations. When the concentration is increased to the point where there is contact between the grains there is a rapid increase in activation energy as illustrated in Figure (2-7). Andersland and Akili [1967] found a value of approximately 100 k. calories/mole for frozen clay. It is assumed that the confinement of the particles by the ice makes the modified rate equation (5-8) relevant in

this case. The value of the hydrostatic pressure exerted by the ice in resisting the movement of the grains is not readily determined, but a check calculation will be made to establish the order of magnitude which would be required.

From equation (5-8)

$$\Delta F = RT\left((\tau - 0.35\sigma_{oct.})V_f/2kT\right) - RT\ell n\frac{kT}{h} - RT\ \ell n\ \gamma \qquad (5\text{-}10)$$

Selecting one of the reported test results which yields a value of 112 k. calories/mole at a creep rate of 2.5×10^{-4} and a temperature of -15°C was selected. The value of 112 k. calories/mole represents an excess of approximately 55 over the combined energies of the ice and clay and if this is to be explained entirely in terms of the confining pressure, the effect of the term $0.35\sigma_{oct}$ must be to reduce the energy by 55 k. calories/mole. Thus

$$0.35\sigma_{oct}\ RV_v/2k = 55{,}000$$

or

$$\sigma_{oct} = 22 \times 10^6 \text{ dynes/sq. cm.}$$

$$= 319 \text{ lb./sq. in.}$$

which is of the order of magnitude which would be expected.

While this approach is considered logical for sands, its application to clays may have to be further modified until more is known about molecular exchange activity at the depressed temperatures. Although it is now believed that a supercooled liquid phase does exist around the particles, the site activity would be greatly reduced and the true free energy of activation may probably be only that of the ice.

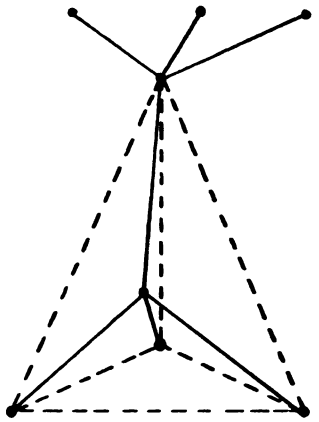

Structure of oxygen atoms in ice lattice
Hydrogen atoms lie in the bonds.

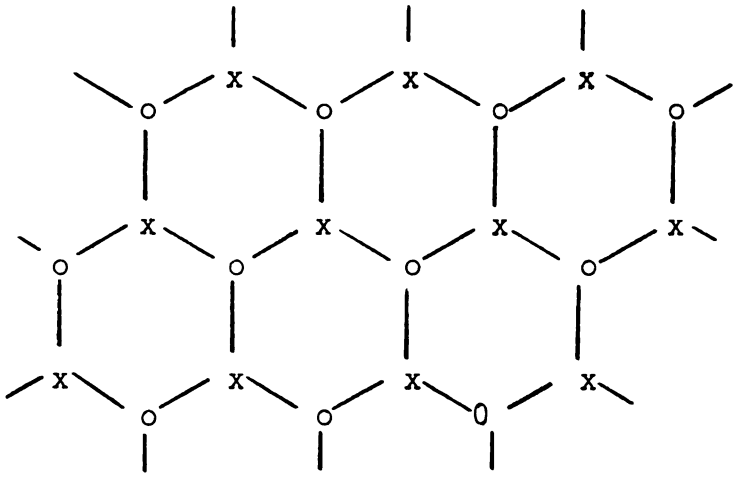

Projection of ice lattice on basal plane;
circles and crosses indicate oxygen atoms
on different planes.

Fig. 5-1. Structure of ice (after Pounder, 1965).

CHAPTER VI

SUMMARY AND CONCLUSIONS

The free energy of activation of Sault Ste. Marie Clay was determined for both viscous flow and secondary creep situations. The clay was treated to remove the carbonates then divided into three batches which were saturated with lithium, sodium, or potassium ions. Portion of each monionic batch was heated to 165° C for seven days and then mixed with carbon tetrachloride to remove the adsorbed water layer.

The viscosity of the three soil-water mixtures increased slowly with increasing concentration of solids until there were sufficient solids present to form a continuous structure. Once a structure had developed, the mixtures became thixotropic and the viscosity increased rapidly. Analysis of the viscosity tests was confined to the region of low concentration. It was found that the lithium saturated soil recorded the highest viscosity and the potassium saturated the lowest at any given concentration. This is related to the different degrees of hydration of the three ions. The greater degree of hydration of the lithium ions increased the effective size of the particles and decreased the partial volume of the free water resulting in a higher viscosity reading.

The free energy of activation was determined by repeating the viscosity tests at three different temperatures, 25, 35, and 45° C. It was found that in the region where the particles do not form a continuous structure, there was no change in the free energy from that of water. Hence the flow mechanism involved is that of free water moving in an increasingly restricted space and that the isolated particles made no contribution to the free energy of activation.

Remoulded samples of each soil, including those saturated with carbon tetrachloride were consolidated in triaxial cells at pressures of 1.75, 3.5, and 7.0 Kg/sg. cm. They were then lightly loaded and when secondary creep was established, additional load increments were applied. This procedure provided sufficient data for the calculation of the free energy of activation and the volume of the flow unit.

The free energy of activation was found to be approximately 28 K. calories/mole and there was no indication of any variation with either the nature of the adsorption complex or the degree of consolidation. The bonding mechanism is therefore not related to the adsorpted water layer but is direct mineral to mineral contact with the formation of ionic bonds at the points of contact. Increased consolidation apparently increases the number of contacts but does not affect the contacts already formed.

The flow volumes derived directly from the experimental data were corrected for the fact that in a particulate medium there is a finite number of contacts and the stress on each contact is therefore greater than the stress calculated on the gross area of the specimen. It was then found that the flow volume was approximately 1.7 cubic angstroms which indicates that the bond is of atomic dimensions. There was a small decrease in the size of the flow unit with increasing density due to the increase in the number of contacts and improvement of the contact junctions.

Application of the rate process theory to sands in both the frozen and unfrozen states was considered and it was concluded that a correction would be needed to allow for the mechanical energy involved in moving the grains against the external forces. The form of this correction was derived.

BIBLIOGRAPHY

BIBLIOGRAPHY

Akili, W. "Stress Effect on Creep Rates of a Frozen Clay Soil from Standpoint of Rate Process Theory." Unpublished Ph.D. dissertation, Michigan State University, 1966.

Al-Nouri, I. "Time Dependent Strength Behavior of Two Soil Types at Lowered Temperatures." Unpublished Ph.D. dissertation, Michigan State University, 1969.

Andersland, O. B. and Akili, W. "Stress Effect on Creep Rates of a Frozen Clay Soil." Geotechnique, Vol. XVII, No. 1 (March, 1967), pp. 27-39.

Baver, L. D. Soil Physics. New York: John Wiley and Sons, 1956

Christensen, R. W. and Wu, T. H. "Analysis of Clay Deformation as a Rate Process." Proc. 4147. Journal of Soil Mech. and Found. Eng. Div., Amer. Soc. of Civil Engineers (November, 1964), pp. 125-157.

Dillon, H. B. and Andersland, O. B. "Deformation Rates of Polycrystalline Ice." Internat. Conf. on Physics of Snow and Ice, The Inst. of Low Temp. Sci., Hokkaido Univ., Sapporo, Japan, August, 1967.

Dorn, J. E. "The Spectrum of Activation Energies for Creep." Creep and Recovery, The American Society of Metals, Cleveland, Ohio (1957), pp. 255-283.

Dorn, J. E. "Creep and Fracture of Metals at High Temperatures." Proc. of Symposium of National Physical Lab. London: Her Magesty's Stationery Office, 1959.

Glasstone, S. Textbook of Physical Chemistry. New York: D. Van Nostrand Co., Inc., 1959.

Glasstone, S., Laidler, K. J. and Eyring, H. The Theory of Rate Processes. New York: McGraw-Hill Book Co., Inc., 1941.

Gold, L. W. "Deformation Mechanisms in Ice." Ice and Snow, Properties, Processes and Applications. Edited by W. D. Kingery. Cambridge, Mass.: MIT Press, 1963.

Goughnour, R. R. "The Soil-Ice System and the Shear Strength of Frozen Soils." Unpublished Ph.D. dissertation, Michigan State University, 1967.

Goughnour, R. R. and Andersland, O. B. "Mechanical Properties of a Sand-Ice System." Journal of the Soil Mech. and Found. Div., Amer. Soc. of Civil Engineers, Paper 6030, SM4, July, 1968.

Grim, R. E. Clay Minerology. New York: McGraw-Hill Book Co., Inc., 1953.

Herrin, M. and Jones, G. E. "The Behaviour of Bituminous Materials from the Viewpoint of the Absolute Rate Theory." Proc. Association of Asphalt Paving Technologists, Vol. 32 (1963), pp. 82-101.

Kauzmann, W. "Flow of Solid Metals from the Standpoint of the Chemical Rate Theory." Trans. Amer. Institute of Mining and Metallurgical Engr., Vol. 143 (1941), pp. 57-83.

Kruyt, H. R. Colloid Science. Vol. I. New York: Elsevier Publishing Co., 1952.

Lambe, T. W. "A Mechanistic Picture of Shear Strength in Clay." Amer. Soc. of Civil Engineers Research Conference on Shear Strength of Cohesive Soils (1960), pp. 555-580.

Low, P. F. and Anderson, D. M. "The Partial Specific Volume of Water in Bentonite Systems." Proc. Soil Science Soc. Amer., Vol. 22 (1958), pp. 22-24.

Low, P. F. and Anderson, D. M. "The Density of Water Adsorbed by Lithium, Sodium and Potassium Bentonite," Vol. 22, 1958.

Marshall, C. E. The Physical Chemistry and Minerology of Soils. New York: John Wiley and Sons, Inc., 1964.

Mellor, M. and Smith, J. M. "Creep of Snow and Ice." Internat. Conf. on Physics of Snow and Ice. The Inst. of Low Temp. Sci., Hokkaido Univ., Sapparo, Japan, August, 1967.

Mitchell, J. K., Campanella, R. G., and Singh, A. "Soil Creep as a Rate Process." Journal of the Soil Mech. and Found. Div., Amer. Soc. of Civil Engineers, January, 1968.

Murayama, S. and Shibata, T. "Rheological Properties of Clays." Proc. 5th Internat. Conf. on Soil Mech. and Found. Eng., Paris, 1961, pp. 269-273.

Nadai, A. Theory of Flow and Fracture of Solids. Vol. 2. New York: McGraw-Hill Book Co., Inc., 1963.

Pounder, E. R. The Physics of Ice. Oxford: Pergamon Press, 1965.

Rosenquist, I. Th. "Physical-Chemical Properties of Soils: Soil-Water Systems." Journal of the Soil Mech. and Found. Div., Amer. Soc. of Civil Engineers, Vol. 85 (1959).

Scott, R. F. Principles of Soil Mechanics. Reading: Addison-Wesley Publishing Co., Inc., 1963.

Singh, A. and Mitchell, J. K. "General Stress-Strain-Time Function for Soils." Journal of the Soil Mech. and Found. Div., Amer. Soc. of Civil Engineers, Paper 5728, SM1, January, 1968.

Thurston, C. W. and Deresiewicz, H. "Analysis of a Compression Test of a Model of a Granular Medium." Trans. Amer. Soc. of Mech. Engineers, Vol. 81 (1959).

van Olphen, H. An Introduction to Clay Colloid Chemistry. New York: Interscience Publishers, 1965.

Verwey, E. J. W. and Overbeek, J. Th. G. Theory of Stability of Lyophobic Colloids. Amsterdam: Elsevier Publishing Co., 1948.

APPENDICES

APPENDIX TABLE I.--Viscosity of Soil-Water Mixtures.

Temperature = 25°C		Temperature = 35°C		Temperature = 45°C	
Concentration g./litre	Viscosity Centipoise	Concentration g./litre	Viscosity Centipoise	Concentration g./litre	Viscosity Centipoise
		Lithium Saturated Clay			
5.32	1.20	8.12	0.95	7.57	0.80
12.26	1.23	14.37	1.02	16.02	0.85
22.40	1.28	31.62	1.10	37.31	0.92
63.94	1.65	72.51	1.41	73.62	1.25
137.53	3.1	128.20	2.30	141.24	2.33
309.33	35.0*	273.80	10.35	252.19	8.00
		Sodium Saturated Clay			
7.02	1.15	6.85	0.92	8.25	0.77
17.10	1.18	15.12	1.00	18.47	0.84
49.81	1.37	37.33	1.13	52.39	0.97
125.22	2.11	94.66	1.35	111.64	1.33
285.76	7.50	181.29	2.52	231.75	3.05
410.37	40.00*	342.81	10.03	372.69	11.00
		Potassium Saturated Clay			
6.07	1.07	9.73	0.93	11.04	0.70
14.12	1.10	23.15	1.00	21.62	0.78
57.30	1.18	77.81	1.11	52.43	0.935
118.25	1.77	116.21	1.42	110.69	1.05
421.82	4.21	381.48	3.79	273.25	1.52
605.10	12.80*	640.34	8.92	580.50	3.81
708.62	44.50*	758.00	36.50*	810.00	47.50*

*At this concentration the viscosity reading was time-dependent. The tabulated figure was read after one minute.

APPENDIX TABLE II.--Creep Test Data for Soil-Water Samples.

	σ_3 = 1.75 kg./sq. cm.		σ_3 = 3.5 kg./sq. cm.		σ_3 = 7.0 kg./sq. cm.	
			Lithium Saturated Clay			
Time mins.	natural strain $x10^{-4}$	natural strain rate $x10^{-4}$/min	natural strain $x10^{-4}$	natural strain rate $x10^{-4}$/min	natural strain $x10^{-4}$	natural strain rate $x10^{-4}$/min
	Axial Stress = 0.83 kg./sq. cm.		Axial Stress = 1.25 kg./sq. cm.		Axial Stress = 1.66 kg./sq. cm.	
0.25	2.2	8.8	2.3	9.2	3.5	16.0
0.50	3.7	6.0	3.8	6.0	5.9	9.6
1	5.2	3.0	5.3	3.0	8.3	4.8
2	9.4	3.2	8.0	2.7	10.7	2.4
4	14.3	2.5	11.1	1.5	13.5	1.4
6	18.9	2.3	13.0	1.0	15.9	0.80
8	21.9	1.5	14.6	0.80	17.5	0.60
10	25.0	1.4	16.1	0.70	18.6	0.50
15	30.3	1.1	20.7	0.90	21.0	0.40
30	41.2	0.72	24.6	0.26	26.6	0.30
45	49.3	0.54	28.9	0.30	30.6	0.20
60	54.5	0.34	32.7	0.25	33.7	0.10
	Stress Increment = 0.104 kg./sq. cm.		Stress Increment = 0.208 kg./sq. cm.		Stress Increment = 0.416 kg./sq. cm.	
60.25	57.2	10.8	35.3	10.4	39.7	24.0
60.50	57.9	2.8	36.1	0.8	41.3	1.6
61	58.7	1.6	36.5	0.8	41.3	1.6
62	59.9	1.2	37.6	1.1	42.5	1.2
64	61.8	0.95	39.2	0.80	44.5	1.0
66	63.3	0.75	40.4	0.60	46.1	0.80
68	64.8	0.75	41.5	0.50	47.3	0.70
70	66.4	0.80	42.3	0.40	48.5	0.60
75	70.2	0.75	45.0	0.18	50.9	0.50
90	77.8	0.50	50.1	0.34	56.9	0.40
105	84.6	0.45	54.6	0.30	60.9	0.30
120	89.6	0.33	58.1	0.23	65.3	0.25
120.25	92.7	12.4	61.2	12.4	70.9	22.4
120.50	93.1	1.6	62.0	3.2	72.0	4.4
121	93.8	1.4	62.8	1.6	73.2	2.4
122	95.3	1.5	63.6	0.8	75.3	2.1
124	96.8	0.75	65.1	0.75	77.7	1.2
126	98.8	1.0	66.7	0.8	80.4	1.3
128	100.3	0.75	68.2	0.75	82.4	1.0
130	101.8	0.75	69.4	0.60	84.0	0.80
135	104.9	0.60	72.0	0.50	88.5	0.80
150	113.3	0.55	78.7	0.45	97.3	0.58
165	120.2	0.46	84.0	0.35	105.0	0.50
180	126.7	0.43	88.3	0.29	109.7	0.31

APPENDIX TABLE III.--Creep Test Data for Soil-Water Samples.

Sodium Saturated Clay

	σ_3 = 1.75 kg./sq. cm.		σ_3 = 3.5 kg./sq. cm.		σ_3 = 7.0 kg./sq. cm.	
Time mins.	Natural strain x 10^{-4}	natural strain rate x10^{-4}/min	natural strain x 10^{-4}	natural strain rate x10^{-4}/min	natural strain x 10^{-4}	natural strain rate x10^{-4}/min
	Axial Stress = 0.83 kg./sq. cm.		Axial Stress = 1.25 kg./sq. cm.		Axial Stress = 1.66 kg./sq. cm.	
0.25	17.0	68.0	4.4	17.6	3.7	14.8
0.50	28.4	45.6	7.7	14.2	6.2	10.0
1	39.4	22.0	11.4	7.4	8.3	4.2
2	53.1	13.7	15.9	4.5	10.4	2.1
4	70.3	8.6	21.7	2.9	12.9	1.25
6	81.2	5.5	25.8	2.0	15.4	1.20
8	89.7	4.3	28.6	1.4	17.1	0.80
10	96.9	3.6	31.1	1.25	18.4	0.65
15	109.9	2.6	35.5	0.90	21.7	0.30
30	134.1	1.6	46.3	0.70	28.7	0.46
45	149.1	1.0	53.7	0.50	33.9	0.35
60	159.4	0.7	59.4	0.35	38.5	0.30
	Stress Increment = 0.104 kg./sq. cm.		Stress Increment = 0.208 kg./sq. cm.		Stress Increment = 0.416 kg./sq. cm.	
60.25	165.2	23.2	64.8	21.6	44.4	23.6
60.50	166.3	4.4	65.6	3.2	45.2	3.2
61	168.3	4.0	67.2	3.2	46.5	2.6
62	170.9	2.6	69.3	2.1	48.2	1.7
64	176.3	2.7	72.1	1.4	50.7	1.2
66	181.0	2.3	75.0	1.45	53.2	1.2
68	184.8	1.9	77.5	1.25	55.8	1.3
70	188.3	1.8	79.6	1.00	57.0	0.60
75	196.8	1.7	83.6	0.80	60.3	0.60
90	215.8	1.3	95.2	0.80	68.4	0.55
105	228.9	0.87	102.7	0.50	75.1	0.45
120	238.9	0.67	108.9	0.40	80.2	0.35
120.25	244.0	20.4	114.7	23.2	86.5	25.2
120.50	--	--	115.9	4.8	87.7	4.8
121	246.7	3.6	117.6	3.4	89.9	4.4
122	249.9	3.2	119.6	2.0	92.4	1.2
124	254.8	2.5	123.8	2.1	97.0	2.3
126	259.1	2.2	127.1	1.6	100.4	1.7
128	263.0	2.0	130.0	1.5	103.4	1.5
130	266.7	1.8	132.9	1.5	106.0	1.3
135	275.1	1.7	138.6	1.15	111.9	1.2
150	295.7	0.4	152.8	0.94	124.1	0.80
165	310.5	1.0	163.2	0.76	133.8	0.65
180	321.9	0.76	172.7	0.57	141.0	0.50

APPENDIX TABLE IV.--Creep Test Data for Soil-Water Samples.

Potassium Saturated Clay

	σ_3 = 1.75 kg./sq. cm.		σ_3 = 3.5 kg./sq. cm.		σ_3 = 7.0 kg./sq. cm.	
Time mins.	natural strain x 10^{-4}	natural strain rate x10^{-4}/min	natural strain x 10^{-4}	natural strain rate x10^{-4}/min	natural strain x 10^{-4}	natural strain rate x10^{-4}/min
	Axial Stress = 0.83 kg./sq. cm.		Axial Stress = 1.75 kg./sq. cm.		Axial Stress = 1.66 kg./sq. cm.	
0.25	10.3	41.2	2.9	11.6	10.0	40.0
0.50	17.6	29.2	4.4	6.0	15.5	22.0
1	26.1	17.0	6.6	0.5	19.1	5.2
2	33.4	7.3	9.9	1.1	21.6	3.4
4	41.6	4.1	7.4	0.75	25.5	2.0
6	--	--	8.6	0.60	28.5	1.5
8	49.4	1.95	9.3	0.35	30.8	1.2
10	--	--	10.1	0.40	32.6	0.90
15	57.9	1.20	11.2	0.22	36.2	0.90
30	65.6	0.55	14.9	0.25	43.7	0.50
45	70.1	0.37	16.4	0.10	48.6	0.33
60	74.1	0.27	18.0	0.10	52.7	0.27
	Stress Increment = 0.104 kg./sq. cm.		Stress Increment = 0.208 kg./sq. cm.		Stress Increment = 0.416 kg./sq. cm.	
60.25	77.5	13.8	20.8	3.5	61.2	34.0
60.5	77.9	3.6	20.4	1.6	63.1	7.6
61	78.6	1.4	21.0	0.60	66.4	6.5
62	79.7	1.1	21.7	0.70	70.6	4.2
64	81.6	1.0	22.5	0.40	76.6	3.1
66	83.1	0.75	23.2	0.35	81.0	2.1
68	85.0	0.50	24.0	0.40	86.9	1.3
70	86.0	0.50	24.0	0.20	86.9	1.3
75	89.0	0.60	25.1	0.22	92.2	1.06
90	95.4	0.40	27.7	0.20	102.6	0.70
105	100.1	0.30	30.0	1.15	108.6	0.40
120	103.1	0.20	31.5	0.10	113.4	0.32
120.25	106.0	11.6	32.6	4.4	122.8	37.6
120.50	106.4	1.6	33.3	2.8	126.2	13.6
121	107.2	1.6	34.0	1.4	131.0	19.2
122	108.7	1.5	34.8	0.80	133.1	7.1
124	110.9	1.1	35.9	0.55	148.0	4.7
126	113.2	1.1	36.7	0.40	155.5	3.5
128	--	--	37.4	0.35	160.7	2.6
130	116.8	0.90	38.2	0.40	164.8	2.0
135	119.9	0.60	39.3	0.22	172.8	1.6
150	127.7	0.52	42.3	0.20	172.8	1.6
165	--	--	45.0	0.13	193.9	0.50
180	--	--	46.5	0.10	196.8	0.33

APPENDIX TABLE V.--Creep Test Data for Soil-Carbon Tetrachloride Samples.

Lithium Saturated Clay						
	σ_3 = 1.75 kg./sq. cm.		σ_3 = 3.5 kg./sq. cm.		σ_3 = 7.0 kg./sq. cm.	
Time mins.	natural strain x 10^{-4}	natural strain rate x10^{-4}/min	natural strain x 10^{-4}	natural strain rate x10^{-4}/min	natural strain x 10^{-4}	natural strain rate x10^{-4}/min.
	Axial Stress = 0.83 kg./sq. cm.		Axial Stress = 1.25 kg./sq. cm.		Axial Stress = 1.66 kg./sq. cm.	
0.25	3.0	12.0	1.1	4.4	1.5	6.0
0.50	5.3	9.2	2.3	4.8	2.7	4.8
1	8.0	5.4	4.2	3.8	4.3	3.2
2	11.4	3.4	6.1	1.9	5.9	1.6
5	17.9	2.2	10.8	1.56	9.8	1.3
10	25.2	1.46	15.4	0.90	13.8	0.80
15	30.2	1.00	18.9	0.70	17.0	0.64
20	34.3	0.80	22.0	0.60	19.7	0.54
30	40.9	0.66	26.7	0.47	24.5	0.48
40	45.5	0.46	30.9	0.42	28.1	0.36
50	49.4	0.39	34.0	0.31	31.2	0.31
60	52.8	0.34	36.7	0.27	34.0	0.28
	Stress Increment = 0.104 kg./sq. cm.		Stress Increment = 0.208 kg./sq. cm.		Stress Increment = 0.416 kg./sq. cm.	
60.25	53.9	4.4	39.1	9.6	37.9	15.6
60.50	54.3	1.6	39.5	1.6	38.3	1.6
61	54.7	0.80	39.9	0.80	38.7	1.6
62	55.0	0.30	40.6	0.70	39.9	1.2
65	56.6	0.50	43.0	0.80	41.9	0.67
70	58.9	0.46	46.1	0.90	45.1	0.64
75	61.2	0.46	48.8	0.54	47.9	0.56
80	--	--	51.2	0.48	50.3	0.48
90	66.3	0.34	55.0	0.38	53.8	0.38
100	69.3	0.30	58.5	0.35	57.4	0.36
110	72.0	0.27	61.6	0.31	60.6	0.32
120	74.7	0.27	64.4	0.28	62.6	0.20
120.25	76.2	6.0	66.7	9.2	65.4	11.2
120.50	76.2	0	67.1	1.6	65.8	1.6
121	76.6	0.80	67.5	0.80	67.8	1.2
122	77.0	0.40	68.3	0.80	67.8	1.2
125	78.6	0.53	70.6	0.74	70.2	0.80
130	80.5	0.42	73.7	0.60	73.7	0.70
135	82.8	0.46	77.2	0.70	76.5	0.56
140	84.7	0.40	79.2	0.40	78.9	0.48
150	88.2	0.35	83.8	0.46	83.7	0.48
160	91.3	0.31	87.7	0.41	87.3	0.36
170	94.0	0.27	91.3	0.36	90.5	0.32
180	96.2	0.22	94.4	0.31	93.3	0.28

APPENDIX TABLE VI.--Creep Test Data for Soil-Carbon Tetrachloride Samples

Sodium Saturated Clay

	σ_3 = 1.75 kg./sq. cm.		σ_3 = 3.5 kg./sq. cm.		σ_3 = 7.0 kg./sq. cm.	
Time mins.	natural strain x 10^{-4}	natural strain rate x10^{-4}/min	natural strain x 10^{-4}	natural strain rate x10^{-4}/min	natural strain x 10^{-4}	natural strain rate x10^{-4}/min
	Axial Stress = 0.83 kg./sq. cm.		Axial Stress = 1.25 kg./sq. cm.		Axial Stress = 1.66 kg./sq. cm.	
0.25	3.0	12.0	1.5	6.0	3.1	12.4
0.50	4.9	7.6	2.7	4.8	5.1	8.0
1	6.9	4.0	3.8	2.2	6.7	3.2
2	10.9	3.8	5.4	1.6	9.1	2.4
5	17.2	2.2	8.1	0.90	13.5	1.5
10	24.2	1.4	10.8	0.54	18.6	1.0
15	29.6	1.08	13.2	0.48	22.2	0.72
20	33.3	0.74	15.1	0.38	25.4	0.64
30	39.9	0.66	18.2	0.31	30.9	0.55
40	44.6	0.47	21.0	0.28	35.3	0.44
50	48.4	0.38	23.7	0.27	39.3	0.40
60	51.1	0.27	26.0	0.23	42.9	0.36
	Stress Increment = 0.104 kg./sq. cm.		Stress Increment = 0.208 kg./sq. cm.		Stress Increment = 0.416 kg./sq. cm.	
60.25	53.5	9.2	28.4	9.6	48.1	20.8
60.50	53.9	1.6	28.8	1.6	48.9	3.2
61	54.2	0.60	29.2	0.80	50.1	2.4
62	54.5	0.30	30.0	0.80	51.3	1.2
65	56.1	0.53	31.8	0.60	54.0	0.90
70	58.0	0.38	34.5	0.54	58.0	0.80
75	--	--	36.5	0.40	--	--
80	61.9	0.39	38.5	0.40	64.0	0.55
90	64.6	0.27	42.0	0.15	68.9	0.49
100	67.0	0.24	44.7	0.19	72.4	0.39
110	69.3	0.23	47.1	0.24	76.4	0.33
120	70.9	0.16	49.4	0.23	79.2	0.35
120.25	72.3	5.6	52.6	12.8	83.7	18.0
120.50	72.5	0.80	53.0	1.6	84.4	2.8
121	72.7	0.40	53.6	1.2	85.2	1.6
122	73.1	0.40	54.4	0.80	86.4	1.2
125	74.3	0.40	56.4	0.67	89.6	1.1
130	76.2	0.34	59.9	0.70	93.7	0.82
135	77.4	0.24	62.7	0.56	96.8	0.62
140	78.9	0.30	64.7	0.40	99.6	0.56
150	81.3	0.24	68.6	0.39	105.3	0.53
160	83.1	0.18	72.0	0.34	108.8	0.39
170	85.1	0.20	74.8	0.28	--	--
180	87.0	0.19	78.0	0.32	115.6	0.68

APPENDIX TABLE VII.--Creep Test Data for Soil-Carbon Tetrachloride Samples.

Potassium Saturated Clay

	σ_3 = 1.75 kg./sq. cm.		σ_3 = 3.5 kg./sq. cm.		σ_3 = 7.0 kg./sq. cm.	
Time mins.	natural strain x 10^{-4}	natural strain rate x10^{-4}/min	natural strain x 10^{-4}	natural strain rate x10^{-4}/min	natural strain x 10^{-4}	natural strain rate x10^{-4}/min
	Axial Stress = 0.83 kg./sq. cm.		Axial Stress = 1.25 kg./sq. cm.		Axial Stress = 1.66 kg./sq. cm.	
0.25	0.7	2.8	0.70	2.8	1.1	4.4
0.50	1.4	2.8	1.5	6.0	1.9	3.2
1	2.9	3.0	2.6	2.2	3.8	3.7
2	9.6	6.7	4.5	1.90	5.7	1.9
5	21.4	3.9	8.6	1.37	9.9	1.4
10	25.9	0.90	11.6	0.60	13.4	0.70
15	27.7	0.36	13.5	0.38	16.5	0.62
20	28.5	0.16	15.0	0.30	18.0	0.30
30	29.6	0.11	17.3	0.23	20.7	0.27
40	30.6	0.10	19.2	0.16	23.0	0.23
50	32.8	0.22	20.3	0.14	24.6	0.16
60	33.9	0.14	21.4	0.11	25.7	0.11
	Stress Increment = .104 kg./sq. cm.		Stress Increment = 0.208 kg./sq. cm.		Stress Increment = 0.416 kg./sq. cm.	
60.25	--	--	23.0	6.14	27.6	3.8
60.50	35.8	7.6	23.3	1.2	28.0	1.6
61	35.8	0.0	23.5	0.40	28.4	0.80
62	36.2	0.40	23.9	0.40	29.2	0.80
65	36.2	0.0	25.2	0.40	32.2	1.0
70	37.3	0.22	--	--	32.2	0.0
75	37.7	0.08	27.1	0.24	33.7	0.30
80	38.0	0.06	28.5	0.28	35.3	0.30
90	38.8	0.08	30.4	0.19	37.6	0.23
100	39.2	0.04	31.9	0.15	39.1	0.15
110	39.3	--	33.5	0.16	40.7	0.20
120	39.5	0.03	34.6	0.11	41.8	0.11
120.25	40.6	4.4	35.7	4.4	43.4	6.4
120.50	40.8	0.80	36.1	1.6	43.8	1.6
121	40.9	0.20	36.3	0.40	44.2	0.80
122	41.8	0.90	36.9	0.60	44.5	0.30
125	42.1	0.10	38.0	0.37	46.1	0.50
130	42.5	0.08	39.9	0.27	48.0	0.38
135	42.9	0.08	--	--	49.6	0.32
140	43.3	0.08	41.8	0.24	50.7	0.22
150	43.6	0.03	43.3	0.15	52.7	0.20
160	44.0	0.04	45.2	0.19	54.5	0.18
170	44.4	0.04	46.0	0.08	55.7	0.12
180	44.6	0.02	47.5	0.15	56.8	0.11